We are grateful to the evaluations from the reviewers, which have allowed us to clarify and improve the manuscript. Below we addressed the reviewer comments, with the reviewer comments in italic and our response in bold.

J.Quaas (Referee #1)

Received and published: 7 November 2017

Bai et al. present a comprehensive calculation of statistics of precipitation vs. aerosol index/cloud droplet concentration from A-Train satellite retrievals. The document differences in the linear regression metrics when applying different (microwave vs. visible-near infrared) LWP retrievals; different precipitation retrievals (albeit all from CloudSat), different aerosol metrics (aerosol index from different retrievals vs. cloud droplet number concentration estimates), and different thresholds.

Although this work does not provide breakthrough science itself, documenting these differences in a consistent way is useful to the debate. The study is in general performed diligently and is pertinent to ACP

I have two main modifications I recommend, and several specific comments.
I have not highlighted semantic or orthographic mistakes since I assume the Copernicus copy editing will take care of this.

Main remarks:
1. The authors should expand their discussion of the state of the art, especially they need to discuss the various other aerosol-precipitation interactions beyond the "lifetime effect". It is in particular necessary that the authors discuss the role of aerosol scavenging when interpreting the metrics they investigate.
Thanks for your comments! We now added more discussion in Section 4 to acknowledge aerosol-precipitaiton interactions beyond the "lifetime effects", and it reads: "It should be noted that precipitation susceptibility in our study is based on Eq. (7) and is derived by linear regression between precipitation fields and CDNC/AI in log-log space. The negative/positive correlation between precipitation frequency/intensity and aerosols may not be readily explained as aerosol effects on precipitation. For example, a negative correlation between precipitation frequency and aerosols may come from the wet scavenging effects of aerosols (more precipitation leads to less aerosols) but not aerosol suppression of precipitation. However, in our study, we not only calculate precipitation susceptibility with respect to AI (S_{X_AI}), but also with respect to CDNC (S_{X_CDNC}) and the later one is expected to be less affected by the wet scavenging effects. The broad consistency between these two estimates shown in our results (Fig. 13), especially for the estimate of S_{POP}, lends the support to the limited

influence of wet scavenging in our estimate. Further support for this comes from the fact that precipitation susceptibility estimates based on the 1 degree L3 MODIS aerosol products are similar to those based on the 10 km L2 MODIS aerosol products (Fig. 4), as we would expect the wet scavenging effects are more important at smaller scales if the wet scavenging effects are a dominating factor. Nevertheless, the effects of wet scavenging can still be important in satellite studies of aerosol-cloud-precipitation interactions, and should be better quantified in future, perhaps in combination with model simulations.".

2. I am a bit astonished on how rather poorly the figures are done. The authors should take care revising these so that the content is more readily understandable.
Thanks a lot for your suggestions! We have revised most figures in the paper according to the comments provided by two referees. This includes adding 95% confidence intervals and zero lines to most figures, and narrowing the range of y-axis in most figures.

Specific remarks
1. P1 l15: Here and at a plenty of instances in the text, the relationship between aerosol and precipitation derived from the observations is overly readily interpreted in a cause-effect manner. If only this science was so easy, then a plenty of issues wouldn't exist. I urge the authors to thoroughly revise their text and imply causality only where they can prove it, or at least where they can corroborate cause-effect relationships. Why not interpret a negative aerosol index – POP relationship, for example, as showing the wet scavenging precipitation effect on aerosol?
The sentence is now reformulated to "We find that S_{POP} strongly depends on atmospheric stability, with larger values under more stable environments". We have added more discussion in Section 4 for addressing this issue. See our reply to your main remaks#1.

2. P1 l26: I suggest the authors adapt to the IPCC AR5 language and define the radiative forcing due to aerosol-cloud interactions ("cloud albedo effect") and cloud adjustments (all subsequent modifications). It is necessary that the authors put the "cloud lifetime effect" hypothesis into context of the manifold other hypotheses.
Thanks for this suggestion! We now adapted the IPCC AR5 language in the manuscript. The text in the first paragraph of the introduction now reads "Aerosol-cloud interactions play an important role in the climate system and affect the global energy budget and hydrological cycle. The effective radiative forcing from aerosol-cloud interactions (ERFaci), which includes the instantaneous effect on cloud albedo from changes in cloud condensation nuclei (CCN) or ice nuclei and all subsequent changes to cloud lifetime and thermodynamics, remains one of the largest

uncertainties in our estimates of anthropogenic radiative forcing (Boucher et al., 2013)." We also removed all other references to "cloud lifetime effect" in the manuscript and replaced it by "cloud water response to aerosol perturbations".

3. P2 l4: Also, the relationship would need to be linear (or more generally, of known, universal, monotonic functional form).
Thanks! We agree and now removed this sentence.

4. P4 l17: But L3 is at 1◦, so far from the stated 5 km resolution.
We are sorry for the confusion here. We now further clarified in the revised manuscript about how the collocation among different datasets is done (See the first paragraph in the section 2.1), including 1 degree MODIS L3 dataset. The reason why we used L3 aerosol product is because we would like to examine how aerosol homogeneity might affect the estimate of precipitation susceptibility. This is now added in the first paragraph of Section 2.2.1 and it reads "This MODIS Level 3 dataset has been used in previous studies to examine aerosol-cloud-precipitation interactions (e.g., L'Ecuyer et al., 2009; Wang et al., 2012) and is compared here with results form the MODIS Level 2 aerosol product to examine how aerosol homogeneity might affect precipitation susceptibility estimates.". The comparison between the MODIS L3 and L2 products is documented in details in Section 3.2.

5. P4 l25: again, why the two, and not only the L2 data?
Please see our reply to comment#4.

6. P5 l1: The authors should report exactly how the colocation is done.
Thanks for the suggestion. We now clarified this in Sec 2.1 and the text reads "MODIS cloud product and CPR radar reflectivity observations used in this study are both provided from the Caltrack datasets, which resample observations from many sensors under CALIOP subtrack with the horizontal resolution of 5km (see the website of http://www.icare.univ-lille1.fr/projects/calxtract/products for more information). For other aerosol and cloud products, including MODIS/CALIOP aerosol products and AMSR-E cloud products, they are further collocated into the CALIOP subtracks in the Caltrack dataset. For each CALIOP subtrack, the closest aerosol/ cloud retrieval sample within one-degree grid box (1°×1°) centered at this subtrack is chosen. To reduce the uncertainty in cloud retrievals, only samples where MODIS cloud fraction is equal to 100% are selected. "

7. P5 l5: A discussion of Christensen et al. doi 10.5194/acp-2017-450 would be useful here.

Thanks for bringing this paper to our attention! This is highly relevant to our study and this paper is now added and discussed in the revised manuscript and it reads "Retrievals of aerosol properties from passive sensors and lidar observation are both affected by clouds near the aerosol, and thereby result in overestimation for aerosol property (Chand et al., 2012; Tackett and Di Girolamo, 2009; Christensen et al., 2017). The extent of this overestimation may be different among different sensors, and depends on how far aerosol pixels chosen are from the corresponding cloud pixels (Christensen et al., 2017).".

8. P5 l7: Wood and Hartmann is a good paper, but is it a pertinent reference here?
Thanks! We checked and this is now removed.

9. P5 l12: What is a "pixel" here? A 1-km MODIS cloud retrieval, or rather an aggregated CALTRACK 5 km grid box?
Pixel here is an aggregated CALTRACK 5 km grid box as MODIS cloud product is provided from the Caltrack datasets. Sorry for the confusion. The sentence is reformulated to "To reduce the uncertainty when deriving CDNC, cloud pixels (identified by Caltrack-MODIS cloud product with the horizontal resolution of 5 km) where cloud optical depth is less than 3 and cloud fraction is less than 100% are excluded (Cho et al., 2015; Zhang and Platnick, 2011)."

10. P5 l15: Is this statement tested/implemented? Or is it just taken for granted from the Kubar study?
Thanks! We now examined the percentage of single layer clouds in our study and it is 94%, consistent with Kubar et al. (2009), and we now updated the text and it reads: "Additionally, we limit our analysis to warm clouds by screening cloud pixels with cloud top temperature warmer than 273K. Under these screening criteria, our results show that 94% warm clouds are single layered (93% in Kubar et al., 2009). Therefore, our analysis mainly focuses on single-layer clouds."

11. P6 l29: It is nonsense that LTS is able to clearly distinguish cloud regimes (e.g. Nam and Quaas doi 10.1002/grl.50945). Klein and Hartmann only show that the seasonal cycles of cloud fraction and LTS correlate.
We agreed that it is still a challenging task to find a unique metric to clearly distinguish different cloud regimes. In previous studies, several metrics were applied to define different cloud regimes. For instance, by using LTSS and vertical pressure velocity, Zhang et al., (2016) divided descending regimes into stratocumulus, transitional clouds and trade wind cumulus regimes. Webb et al., (2015) developed an index (ALPI) based on LTSS and precipitation to distinguish cloud regimes.

LTSS may have its limitation for defining different cloud regimes. However, our results show that precipitation susceptibility has clear LTSS-dependence, especially for S_{POP} (Fig 11 and Fig 13). This suggests LTSS provides a feasible way to examine how precipitation susceptibility may depend on cloud regimes. LTSS was also used in many previous studies (e.g.,L'Ecuyer et al., 2009; Terai et al., 2015). Nevertheless, we acknowledged the limitation of LTSS in the revised manuscript in Section 3.6 and it reads: " Our results also suggest that it is important to account for the influence of atmospheric stability owing to the clear dependence of S_{POP} on metrics like LTSS, though it is acknowledged that LTSS alone is an imperfect metric for isolating cloud regimes (e.g., Nam and Quaas, 2013). Different metrics associated with cloud regimes should be examined in future to better understand the effect of cloud regimes on precipitation susceptibility. For instance, LTSS can be combined with vertical pressure velocity to distinguish between different cloud types (Zhang et al., 2016).".

12. P6 l30: The term "unstable" is a misnomer. "unstable" would mean, a negative LTSS.

Given that our study focus on ocean warm clouds mostly with positive LTSS values, we followed the same definition of unstable as L'Ecuyer et al., (2009) and Wang et al., (2012), and they both defined unstable environment by LTSS values less than 13.5K.

13. P7 l10: Why this choice and not deciles?

In our analysis, we keep the LWP bins the same when we compare different satellite products in individual plots in order to facilitate the comparison. So the number of samples for each LWP varies, from 5% to 14%. However, each LWP bin still includes more than ten thousand samples, large enough for producing robust estimate of precipitation susceptibility.

14. P9l5: When using AMSR-E LWP, are the pixels selected overcast at AMSR-E footprint? Or is the AMSR-E interpolated to the CALTRACK grid cells?

The AMSR-E pixels closest to CALTRACK grid cells are selected. We do not require the AMSR-E pixels to be overcast, but clouds from the CALTRACK pixels are overcast with MODIS cloud fraction of 100%. The details of collocation strategy are added to Sec 2.1 in the revised manuscript.

15. P9 l17: Is this may be due to the fact that AMSR-E LWP in fact is cloud fraction times in-cloud LWP, in combination with the fact that CDNC is positively correlated to cloud fraction (Fig. 2)?

Thanks! If this is the case, for a constant AMSR-E LWP shown in Fig. 7f, in-cloud LWP would decrease with increasing CDNC as increasing CDNC means increasing cloud fraction. Smaller in-cloud LWP would then imply lower precipitation intensity, opposite to what is shown in Fig. 7f. Our

results shown in Fig. 8 suggests that this might be related to differences in MODIS and AMSR-E LWP at low MODIS CDNC, but what might cause the discrepancies in two LWP product still needs further investigation in the future.

16. Fig. 1: Since there are only ten bins in LWP, I suggest to label each bin center on the x-axis. Possibly the axis could be chosen irregular then. It would be good to indicate the total amount of data points in the caption. In (a) a zeroline would be helpful.
We have added a zeroline in the Fig. 1. The total number of data points now is included in the caption. Since labels of the x-axis would be dense and overlapped at low LWP if we label each mean value of LWP bin, the x-axis now is divided into smaller intervals. In addition, each mean value of LWP bin is shown in Fig.7.

17. Fig. 4: The authors need to choose a different y-axis that spans only the range of data. As it is now, no details can be distinguished. Again, a zeroline is necessary
The range of y-axis is now narrowed and a zeroline is also added for most figures (Fig.1, Fig.3-Fig.5 and Fig.9-Fig.11)in the revised manuscript.

18. Fig. 5: zeroline would be good
A zeroline is now added in the Fig.5.

19. Fig. 7: a, b, e, f: more x-axis tick marks necessary; e-f: more y-axis tick marks necessary
More x-axis and y-axis tick marks are now added accordingly.

20. Fig. 10 b: zeroline necessary
A zeroline is now added in the Fig.10.

21. Fig. 12: the color code is poorly selected. The colors should be centered around zero (light pink shouldn't indicate positive). Are the LTSS bins chosen so that each contains on average the same amount of pixels (that is the way it should be, else a PDF of LTSS would need to be shown).
We have changed the color code of Fig. 12 and its colors are now centered around zero. The light pink now indicates negative value. In this figure, each LTSS bin now contains on average the same amount of pixels. We also have added this sentence to the caption of Fig. 12.

22. Fig. 14: is it not possible to differentiate likelihoods, e.g. by putting equal weight on each curve entering the shaded area and then varying the color intensity/darkness?
Thanks a lot for your suggestion! We would like to take this suggestion, but as we only have eight curves for each metric shown in Fig. 14, we do not

have large number of curves to show the likelihoods., so we have to keep the figure as it is.

Anonymous Referee #2

Received and published: 11 November 2017

In various studies, the precipitation susceptibility metric has been used to quantify the effect of aerosols on the precipitation in both models and observations and to indicate the strength of the cloud lifetime effect. The present article examines how observationally-based estimates of the precipitation susceptibility metric vary depending on the various dataset and analysis choices. Previous attempts to provide an observational constraint on the precipitation susceptibility metric have led to different strengths in susceptibility and also in different behaviors of the susceptibility. The study contributes to the existing literature by attempting to reconcile those differences by examining a wide range of data and analysis choices in the same framework, which might help answer why different studies have arrived at different susceptibility estimates. The authors examine the sensitivity of the susceptibility metric to the choice of aerosol proxy, precipitation characteristic (intensity, probability of precipitation (POP), or mean precipitation), stability regime, liquid water path retrieval, precipitation retrieval, and precipitation threshold. After examining the whole range of sensitivities, the authors conclude that SPOP has the least amount of spread that arises from the choice of liquid water path and precipitation data product. The authors also find strong sensitivities in the choice of stability regime and in whether aerosol index (AI) or the cloud droplet number concentration (CDNC) is used as the aerosol proxy.

The study is a substantial contribution to the existing literature by providing a comprehensive examination of the possible source of discrepancies that can arise when trying to estimate the precipitation susceptibility based on satellite retrievals. The manuscript methodically goes through the different choices that can be made, and assesses their impact on the value and behavior of the metric. There are a couple issues with the paper that I would like to see the authors address. First, the authors mention in the introduction of how estimates from Wang et al. (2012), Terai et al. (2015), and Michibata et al. (2016) differ in the magnitude of the SPOP metric. Although it appears that the use of AI or CDNC is the largest source of the discrepancy, I expected to see the authors discuss more thoroughly how the effect of the choice of aerosol proxy compares with effect of the choice of precipitation dataset and threshold. I had also expected a similar discussion that folds in the results from Sorroshiaan et al. (2009) on both the magnitude of the susceptibility, as well as the behavior of the susceptibility. Second, statistical confidence limits to the susceptibilities should be provided to determine how the statistical uncertainties compare with the other dataset/methodology uncertainties that are examined in the study. The confidence intervals would help inform whether the

choice of datasets significantly change the susceptibility estimates or not. Overall, the manuscript has a clear scientific question, uses analyses that address the question, and is well organized. I do not consider the main issues that I have to be major. Therefore, I recommend that the manuscript be published after the following comments and issues have been addressed.

Main comments and issues:
1. The uncertainties in the susceptibility estimates should be reported in all the figures and graphs. The 95% confidence intervals can be calculated from the standard deviation of the regression or using bootstrapping techniques. The statistical uncertainties will help the author substantiate some of the statements within the manuscript that say whether or not various choices significantly change the susceptibilities.
The error bars with 95% confidence intervals are now added to all the susceptibilities figures except Fig. 10 and Fig. 11. Given that each panel of Fig. 10 and Fig. 11 includes six susceptibility curves, these figures would be not clear and messy if error bars are added. The error bars can be found for global mean values for these cases in Fig. 13.

We thank the reviewer for this excellent suggestion! Adding the statistical uncertainties indeed helps us substantiate some of our statements in the manuscript. For instance, we can state with confidence that S_{POP} estimates are not significantly influenced by LWP products, while S_I estimates are, as shown in Fig. 5 in the revised manuscript. On the other hand, the differences of dlnCDNC/dlnAI between different stability regimes are not significant (Fig. 3). We also find that almost all of mean S_{I_CDNC} is significantly negative regardless of stability regimes (Fig. 13).

2. Given that the main purpose of the study is to examine how the various choices have led to differences in the susceptibility that are reported in the literature, the authors should provide more discussion on how this study helps to reconcile existing differences. In particular, the authors should do their best to identify likely reasons why the estimates in the previous studies have differed (if they do). For example, there are differences in the magnitude of the susceptibility (e.g., Wang et al., 2012 versus Terai et al., 2015). There are also differences in the behavior of susceptibility (monotonic decrease versus increase and then decrease).
We have provided more discussion on the differences in both magnitude and behavior of susceptibility in previous studies in the second paragraph of the Section 4 (Discussion). Now the text reads "Our results may help to reconcile some of the differences in previous estimates of precipitation susceptibility. For example, our results show that $S_{X\_AI} \approx 0.3 S_{X\_CDNC}$,(Table 3 and Fig. 1), which explains why S_{POP_CDNC} in Terai et al. (2015) is much larger than S_{POP_AI} in Wang et al., (2012). Previous studies are also different in how precipitation susceptibility varies with increasing LWP. Our results

show that S_I generally increases with LWP at low and moderate LWP and then decreases with increasing LWP at moderate and high LWP, consistent with results from Feingold et al., (2013), Michibata et al., (2016) and Jung et al., (2016). The monotonic increase of S_{I_CDNC} with increasing LWP in Terai et al., (2015) is mainly because that the LWP range in their study is relatively narrow (from 0 to ~400 g m^{-2}) and our results suggest that when the upper bound of LWP is extended to ~800 g m^{-2}, the "descending branch" (S decreases with increasing LWP) noted in Feingold et al. (2013) appears, though the exact LWP value where S_{I_CDNC} peaks depend on LWP and rain products used as well as the rainfall threshold choices."

3. The authors seem to argue for the use of SPOP as a metric to quantify aerosol-cloud-precipitation interactions due to SPOP having a smaller range of possible values, based on different LWP and precipitation rate retrievals (Fig. 14). There is less discussion on the advantages and disadvantages of using CDNC or AI as a metric and also a lack of discussion on how the threshold (rain vs. drizzle) can significantly change SPOP values. Given that the authors have examined a wide range of potential sources that lead to differences in susceptibility estimates, it would be informative for the readers to have the authors synthesize their findings and discuss what should be considered in future attempts to try to observationally constrain precipitation susceptibility or attempts to compare susceptibilities from models and from observations.

Thanks for your suggestions! We now made further recommendations on how to better use these metrics to quantify aerosol-cloud-precipitation interactions in models and observations in Section 5, and it reads:

"As S_{POP} demonstrates relatively robust features across different LWP and rain products, this makes it a valuable metric for quantifying aerosol-cloud-precipitation interactions in observations and models. For instance, it would be highly interesting to examine why S_{POP} strongly depends on atmospheric stability and how well this dependence is represented in a hierarchy of models (e.g., large eddy simulations, cloud resolving models, regional climate models, and global climate models). We also note that S_{POP_CDNC} is generally less uncertain compared to S_{POP_AI} and that a relatively robust relationship between S_{POP_CDNC} and S_{POP_AI} exists (i.e., $S_{X\_AI} \approx 0.3 S_{X\_CDNC}$) (Fig. 13 and Table 3). Given that aerosol retrievals near clouds are still challenging and aerosol-cloud relationships in satellite observations can be affected by aerosol retrieval contaminations from clouds, we recommend to first thoroughly quantify S_{POP_CDNC} in observations and models. As S_{POP_CDNC} is derived based on CDNC instead of AI, S_{POP_CDNC} is also not influenced by wet scavenging. Only after S_{POP_CDNC} is thoroughly quantified, we can then combine it with how CDNC depends on AI to better quantify S_{POP_AI}.

On the other hand, S_I estimates strongly depend on satellite retrieval products. Uncertainties in S_I estimate are particular large when S_I is estimated based on rain samples (> 0 dBZ) rather than drizzle samples (> -15 dBZ). It would then be desirable to use drizzle samples to estimate S_I. However, satellite retrieval of precipitation rate for drizzle can be highly uncertain. It is therefore recommended to further improve the retrieval accuracy of precipitation rate for drizzle in satellite observations in order to better use satellite estimate of S_I to quantify aerosol-cloud precipitation interactions. Alternatively, long-term ground and in-situ observations with high accuracy precipitation rate retrievals can be used to provide better estimate S_I and to further quantify aerosol-cloud-precipitation interactions.".

Further discussions are added on difference of S_{POP} and S_I between rain and drizzle in Section 5 and now the text reads " Our results suggest that onset of drizzle is not as readily suppressed by increases in AI or CDNC in warm clouds as rainfall (i.e., S_{POP} is smaller for drizzle than for rain, especially at moderate LWP, Fig. 9). This may partly come from the fact that POP of drizzle is close to 100% at moderate and high LWP regardless of CDNC or AI values (Fig. 7a-d), which makes it insensitive to perturbations in CDNC or AI and results in smaller S_{POP} at these LWP bins compared with S_{POP} for rain (Fig. 9). On the other hand, precipitation intensity susceptibility is generally smaller for rain than for drizzle. This is consistent with our expectation that when precipitation intensity increases, accretion contributes more to the production of precipitation, which makes precipitation intensity less sensitive to perturbation in CDNC or AI, as accretion is less dependent on CDNC compared with autconversion (Feingold et al., 2013; Wood, 2005)"

Minor Comments:
1. P2 L3: "Susceptibility is an inherent property of the aerosol-cloud system." – This is an interesting statement, but it is also vague. Does the statement mean that susceptibility doesn't change with cloud condition? Or aerosol condition? Should they be robust to differences in measurement platform, etc.?
We agree this statement is indeed vague, and this statement is now removed in the revised manuscript.

2. P5 L32: "... selected in close proximity of clouds pixels." What exact criteria is used to determine how close aerosol retrievals must be to be used in the study?
Exact criteria for collocation are added in Sec 2.1. Now the text reads "…. MODIS cloud product and CPR radar reflectivity observations used in this study are both provided from the Caltrack datasets, which resample observations from many sensors under CALIOP subtrack with the horizontal resolution of 5km (see the website of

http://www.icare.univ-lille1.fr/projects/calxtract/products for more information). For other aerosol and cloud products, including MODIS/CALIOP aerosol products and AMSR-E cloud products, these are further collocated into the CALIOP subtracks in the Caltrack dataset. For each CALIOP subtrack, the closest aerosol and cloud retrieval samples within one-degree grid box (1°×1°) centered at this subtrack are chosen. To reduce the uncertainty in cloud retrievals, only samples where MODIS cloud fraction is equal to 100% are selected".

3. P6 L23: replace "significant" with "significantly"
Done.

4. P6 L25: What is the spatial resolution of the precipitation data? Is it at the footprint level? In general, how are pairs of LWP, precipitation rate, and aerosol proxy combined? Are they all combined at the footprint of the precipitation rate? Is the coarsest footprint used for the comparison?
The horizontal resolution of all precipitation data used in the paper is at a footprint level with 1.3km cross track and 1.7 km along track except CPR radar reflectivity observations (i.e., 2B-GEOPROF product collocated to CALIOP subtrack with 5km resolution). The resolution of different products can be seen in Table2. Overall, MODIS LWP, precipitation rate from 2B-GEOPROF and aerosol proxy are combined to CALIOP subtrack since CALIOP aerosol product, MODIS cloud product and CPR 2B-GEOPROF product used in the paper are all provided from Caltrack datasets. For other retrieval products, including MODIS/CALIOP aerosol products and AMSR-E cloud products, these are further collocated into the CALIOP subtracks in the Caltrack dataset. For each CALIOP subtrack, the closest aerosol and cloud retrieval samples within one-degree grid box (1°×1°) centered at this subtrack are chosen. More details can be found in the first paragraph of Sec 2.1 in the revised manuscript.

5. P7 L15: Provide some indication of statistical uncertainty in the estimates in Fig. 1. See main comment 1. Also, it would be informative to indicate the 0 value with a dotted or gray line, because values below that line will indicate that increases in aerosols/cloud droplets lead to more precipitation.
We have added error bars with 95% confidence intervals and zeroline in the Fig. 1.

6. P7 L22-24: The turning point is very slight. The confidence intervals will be helpful in determining how significant the peak is.
Thanks! We now added error bars. The peak is not significant anymore after the error bars are added. But S_{I_CDNC} would decrease distinctly after the peak if the upper bound of LWP and the number of LWP bins both increased (see figure below). The sentence is now reformulated to

"Although the S_{I_CDNC} peak (around 0.6 with LWP 350 gm^{-2}) is not significant in Fig. 1b, S_{I_CDNC} would decrease distinctly after the peak if the upper bound of LWP and the number of LWP bins both increase (not shown). This turning point may correspond to conversion process shifting from the autoconversion to accretion regime (Michibata et al., 2016)."

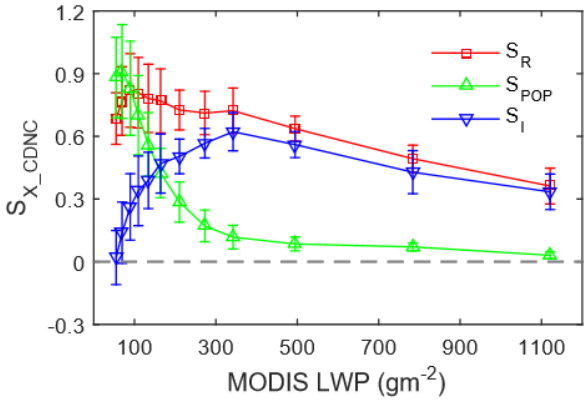

Same as the Fig. 1b but with increase in the upper boundary of LWP and the number of LWP bins

7. P7 L29: To show that the fluctuations in the mean are small compared to noise, the interquartile range (between 25th percentile and 75th percentile) can be shown.
Done. The interquartile range is now added to Fig. 2.

8. P7 L29: Also, because the AI vs. CDNC relationship takes the form d ln(CDNC)/d ln(AI) and because it looks like the AI has a lognormal distribution, it might be better to plot the x-axis in log-scale.
Done. Now the x-axis in Fig. 2 is in log-scale.

9. P8 L4-5: The differences in dlnCDNC/dlnAI between the different stability regimes are interesting, in particular, the lack of sensitivity (or negative sensitivity at high LWPs). Are these differences significant? Do the authors have an explanation as to why the stability affects the sensitivity?
We now add error bars to Fig. 3, and now the differences in dlnCDNC/dlnAI between the different stability regimes and negative sensitivity at high LWP are both not significant anymore.

10. P8 L16: The subtle differences in Fig 4 are hard to see because of the large y-axis range. I can understand the choice to try to keep the same axis range across different figures, but in this case, I would suggest narrowing the range to allow the reader to discern any differences.
We have narrowed the range of y-axis and also added a zeroline to this figure in the revised manuscript.

11. P8 L26-28: Is there a reason why we would rely more heavily on and prefer MODIS AI rather than CALIPSO AI?

This is mainly because MODIS AI has been widely used in previous studies for examining aerosol-cloud-precipitation interactions. What is more, Costantino and Bréon, (2010) shown that AOD estimate from CALIPSO product was very noisy and less reliable than the equivalent parameter from MODIS. The 2D vs. 1D sampling is a likely reason for the MODIS AI being a bit smoother that the CALIPSO AI.

12. P9 L2-7: This is one case where confidence intervals can show that the SPOP estimates are not significantly affected by the choice of LWP retrievals, whereas the SI and SR estimate are significantly affected.

Thanks a lot for this excellent suggestion! After adding error bars to Fig.5, it indeed shows the discrepancies in S_{POP} between MODIS and AMSR-E LWP are not significant. We have added this sentence to the first paragraph in Sec 3.3.

13. P9 L26: Data is plural, so it should be "... when data are binned..."

Corrected.

14. P10 L11: Although the axis labels show this, the figure caption to Figure 9 should indicate the difference between the top row and the bottom row.

We have clarified this in the caption of Fig. 9.

15. P10 L26-28: What is the impact on SR if SPOP increases and SI decreases with increases in the threshold?

S_R is indeed not affected by the rainfall definition since mean rain rate for any given LWP/CDNC or LWP/AI bin is calculated for both rainy and non-rainy clouds, and does not depend on rainfall thresholds used to define a rain event. We have added this sentence to the third paragraph in Sec 3.4 and it reads "By contrast, S_R is not affected by the rainfall definition since the mean rain rate R for a given LWP/CDNC or LWP/AI bin is calculated based on both rainy and non-rainy clouds and does not depend on rainfall thresholds (not shown)."

16. P10 L31: "more significant" should be replaced with "larger", because significant has a particular meaning in the literature (statistical significance), and to state more significant would require examining the confidence intervals.

Done.

17. P11 L28: "sigh" should be replaced by "sign"

Done.

18. P14 L5: Insert "by increases in AI or CDNC" between "readily suppressed" and

"in warm clouds"
Done.

19. P14 L5-6: Taken at face value, this statement is counterintuitive, isn't it? Wouldn't we expect rainfall, which is more dependent on accretion than on autoconversion, to have a weaker dependence to CDNC?
The above expectation is consistent with how S_I changes with rainfall thresholds. When the rainfall threshold increases, it shifts the production of rain from autoconversion to accretion, which reduces precipitation intensity susceptibility. As for precipitation frequency susceptibility, it depends on how often precipitation frequency reaches its upper limit, 100%. As the rainfall threshold decreases from 0 dBZ to -15 dBZ, POP for drizzle is close to 100% at intermediate and high LWP as shown in the figure below, which make it insensitive to perturbation in CDNC or AI at intermediate and high LWP, resulting in much smaller S_{POP} at these LWP bins as shown in Fig. 9 in the main text. We now added this discussion to the third paragraph in Sec.5. Now the text reads "Our results suggest that onset of drizzle is not as readily suppressed by increases in AI or CDNC in warm clouds as rainfall (i.e., S_{POP} is smaller for drizzle than for rain, especially at moderate LWP, Fig. 9). This may partly come from the fact that POP of drizzle is close to 100% at moderate and high LWP regardless of CDNC or AI values (Fig. 7a-d), which makes it insensitive to perturbations in CDNC or AI and results in smaller S_{POP} at moderate and high LWP bins compared with S_{POP} for rain (Fig. 9). On the other hand, precipitation intensity susceptibility is generally smaller for rain than for drizzle. This is consistent with our expectation that when precipitation intensity increases, accretion contributes more to the production of precipitation, which makes precipitation intensity less sensitive to perturbation in CDNC or AI, as accretion is less dependent on CDNC compared with autconversion (Feingold et al., 2013; Wood, 2005). ".

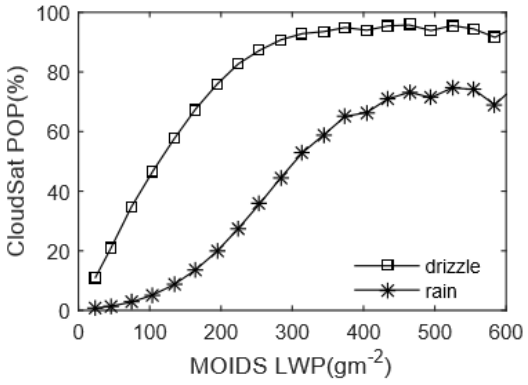

Probability of precipitation as a function of MODIS LWP and its breakdown into drizzle (>0.14 mm d^{-1}) and rain (>2 mm d^{-1})

20. P14 L14: Replace "value" with "values"

Done.

21. P14 L14-18: Are these results consistent with existing conceptual frameworks (such as those based on LES) on how stability affects aerosol-cloud-precipitation interactions? Are there LES studies that have addressed how stability might affect susceptibility?

The pattern of S_{POP_AI} under different stability conditions from our paper (Fig. 13b and Fig. 13f) is consistent with the findings of L'Ecuyer et al., (2009). In addition, Terai et al., (2015) found maximum S_{POP_CDNC} occurred in regions where stable regime is predominant. These satellite-based studies, however, did not provide physical interpretations of such results. Lebo and Feingold (2014) calculated precipitation susceptibility for stratocumulus and trade wind cumulus using large-eddy simulations(LES) and included an overview of precipitation susceptibility estimates in the ligature based on LES. However, their study focus on the relationship between precipitation susceptibility and cloud water response to aerosol perturbations, and did not examine how precipitation susceptibility might be different for clouds under different cloud regimes. We now added this discussion in the revised manuscript and calls further efforts to understand this difference, especially for S_{POP} in the Section 5.

References:

Boucher, O., Randall, D., Artaxo, P., Bretherton, C., Feingold, G., Forster, P., Kerminen, V.-M., Kondo, Y., Liao, H., Lohmann, U., Rasch, P., Satheesh, S. K., Sherwood, S., Stevens, B., and Zhang, X. Y.: Clouds and Aerosols, in: Climate Change 2013: The Phys- ical Science Basis. Contribution ofWorking Group I to the Fifth Assessment Report of the Intergovernmental Panel on Climate Change, edited by: Stocker, T. F., Qin, D., Plattner, G.-K., Tignor, M., Allen, S. K., Boschung, J., Nauels, A., Xia, Y., Bex V., and Midgley, P. M., Cambridge University Press, Cambridge, United Kingdom and New York, NY, USA, 2013.

Albrecht, B. A.: Aerosols,cloud microphysics, and fractional cloudiness, Science (80-.)., 245(4923), 1227–1230, doi:10.1126/science.245.4923.1227, 1989.

Cho, H.-M., Zhang, Z., Meyer, K., Lebsock, M., Platnick, S., Ackerman, A. S., Di Girolamo, L., C.-Labonnote, L., Cornet, C., Riedi, J. and Holz, R. E.: Frequency and causes of failed MODIS cloud property retrievals for liquid phase clouds over global oceans, J. Geophys. Res. Atmos., 120(9), 4132–4154, doi:10.1002/2015JD023161, 2015.

Christensen, M. W., Neubauer, D., Poulsen, C., Thomas, G., McGarragh, G., Povey, A. C., Proud, S. and Grainger, R. G.: Unveiling aerosol-cloud interactions Part 1: Cloud contamination in satellite products enhances the aerosol indirect forcing

estimate, Atmos. Chem. Phys. Discuss., 20(May), 1–21, doi:10.5194/acp-2017-450, 2017.

Duong, H. T., Sorooshian, A. and Feingold, G.: Investigating potential biases in observed and modeled metrics of aerosol-cloud-precipitation interactions, Atmos. Chem. Phys., 11(9), 4027–4037, doi:10.5194/acp-11-4027-2011, 2011.

Feingold, G., McComiskey, A., Rosenfeld, D. and Sorooshian, A.: On the relationship between cloud contact time and precipitation susceptibility to aerosol, J. Geophys. Res. Atmos., 118(18), 10544–10554, doi:10.1002/jgrd.50819, 2013.

L'Ecuyer, T. S., Berg, W., Haynes, J., Lebsock, M. and Takemura, T.: Global observations of aerosol impacts on precipitation occurrence in warm maritime clouds, J. Geophys. Res. Atmos., 114(9), 1–15, doi:10.1029/2008JD011273, 2009.

Lebo, Z. J. and Feingold, G.: On the relationship between responses in cloud water and precipitation to changes in aerosol, Atmos. Chem. Phys., 14(21), 11817–11831, doi:10.5194/acp-14-11817-2014, 2014.

Michibata, T., Suzuki, K., Sato, Y. and Takemura, T.: The source of discrepancies in aerosol--cloud--precipitation interactions between GCM and A-Train retrievals, Atmos. Chem. Phys., 16(23), 15413–15424, doi:10.5194/acp-16-15413-2016, 2016.

Twomey, S.: The Influence of Pollution on the Shortwave Albedo of Clouds, J. Atmos. Sci., 34(7), 1149–1152, doi:10.1175/1520-0469(1977)034<1149:TIOPOT>2.0.CO;2, 1977.

Wang, M., Ghan, S., Liu, X., L'Ecuyer, T. S., Zhang, K., Morrison, H., Ovchinnikov, M., Easter, R., Marchand, R., Chand, D., Qian, Y. and Penner, J. E.: Constraining cloud lifetime effects of aerosols using A-Train satellite observations, Geophys. Res. Lett., 39, L15709, doi:10.1029/2012GL052204, 2012.

Webb, M. J., Lock, A. P., Bretherton, C. S., Bony, S., Cole, J. N. S., Idelkadi, A., Kang, S. M., Koshiro, T., Kawai, H., Ogura, T., Roehrig, R., Shin, Y., Mauritsen, T., Sherwood, S. C., Vial, J., Watanabe, M., Woelfle, M. D. and Zhao, M.: The impact of parametrized convection on cloud feedback, Philos. Trans. R. Soc. A Math. Phys. Eng. Sci., 373(2054), 20140414, doi:10.1098/rsta.2014.0414, 2015.

Wood, R.: Drizzle in Stratiform Boundary Layer Clouds. Part II: Microphysical Aspects, J. Atmos. Sci., 62(9), 3034–3050, doi:10.1175/JAS3530.1, 2005.

Zhang, S., Wang, M., J. Ghan, S., Ding, A., Wang, H., Zhang, K., Neubauer, D., Lohmann, U., Ferrachat, S., Takeamura, T., Gettelman, A., Morrison, H., Lee, Y., T. Shindell, D., G. Partridge, D., Stier, P., Kipling, Z. and Fu, C.: On the characteristics of aerosol indirect effect based on dynamic regimes in global climate models, Atmos. Chem. Phys., 16(5), 2765–2783, doi:10.5194/acp-16-2765-2016, 2016.

Zhang, Z. and Platnick, S.: An assessment of differences between cloud effective particle radius retrievals for marine water clouds from three MODIS spectral bands, J. Geophys. Res. Atmos., 116(20), doi:10.1029/2011JD016216, 2011.

Estimating precipitation susceptibility in warm marine clouds using multi-sensor aerosol and cloud products from A-Train satellites

Heming Bai[1,2], Cheng Gong[3], Minghuai Wang[1,2], Zhibo Zhang[4], Tristan L'Ecuyer[5]

[1]Institute for Climate and Global Change Research and School of Atmospheric Sciences, Nanjing University, Nanjing, China
[2]Collaborative Innovation Center of Climate Change, Jiangsu Province, China
[3]Institute of Atmospheric Physics, Chinese Academy of Science, Beijing, China
[4]Physics Department, University of Maryland Baltimore County (UMBC), Baltimore, Maryland, USA
[5]Department of Atmospheric and Oceanic Sciences, University of Wisconsin, Madison, Wisconsin, USA

Corresponding to: Minghuai Wang (minghuai.wang@nju.edu.cn)

Abstract. Precipitation susceptibility to aerosol perturbation plays a key role in understanding aerosol-cloud interactions and constraining aerosol indirect effects. However, large discrepancies exist in the previous satellite estimates of precipitation susceptibility. In this paper, multi-sensor aerosol and cloud products, including those from CALIPSO, CloudSat, MODIS, and AMSR-E from June 2006 to April 2011 are analyzed to estimate precipitation frequency susceptibility S_{POP}, precipitation intensity susceptibility S_I, and precipitation rate susceptibility S_R in warm marine clouds. We find that S_{POP} strongly depends on atmospheric stability, with larger values under more stable environments. Our results show that precipitation susceptibility for drizzle (with -15 dBZ rainfall threshold) is significantly different from that for rain (with 0 dBZ rainfall threshold). Onset of drizzle is not as readily suppressed in warm clouds as rainfall while precipitation intensity susceptibility is generally smaller for rain than for drizzle. We find that S_{POP} derived with respect to aerosol index (AI) is about one-third of S_{POP} derived with respect to cloud droplet number concentration (CDNC). Overall, S_{POP} demonstrates relatively robust features throughout independent liquid water path (LWP) products and diverse rain products. In contrast, the behaviors of S_I and S_R are subject to LWP or rain products used to derive them. Recommendations are further made for how to better use these metrics to quantify aerosol-cloud-precipitation interactions in observations and models.

dell 2017/12/4 8:41 AM
已删除: stronger reductions in precipitation occurrence observed

1 Introduction

Aerosol-cloud interactions play an important role in the climate system and affect the global energy budget and hydrological cycle. The effective radiative forcing from aerosol-cloud interactions (ERFaci), which includes the instantaneous effect on cloud albedo from changes in cloud condensation nuclei (CCN) or ice nuclei and all subsequent changes to cloud lifetime and thermodynamics, remains one of the largest uncertainties in our estimates of anthropogenic radiative forcing (Boucher et al., 2013). Over the past few decades, numerous methodologies have been developed to understand and quantify the impacts of aerosol-cloud interactions on the climate system. A unique method is to use the so-called "susceptibility" to explain and predict how cloud and precipitation would response if there were some aerosol perturbations. Susceptibility is defined as the

dell 2017/12/8 2:27 PM
已删除: .

derivative of cloud and/or precipitation properties with respect to aerosol related properties. For example, Platnick and Twomey (1994) proposed a cloud albedo susceptibility as $S_\lambda = \partial A/\partial CDNC$, where A is cloud albedo and CDNC is cloud droplet number concentration, to quantify the cloud albedo effect of aerosol.

Precipitation susceptibility has been proposed to evaluate aerosol-cloud-precipitation interactions and to further constrain cloud water response to aerosol perturbations in climate models (Feingold and Siebert, 2009; Terai et al., 2012; Wang et al., 2012). It was first proposed by Feingold and Siebert (2009) and was defined as:

$$S_0 = -\frac{d\ln R}{d\ln CDNC} \quad (1)$$

where R is precipitation intensity (precipitation rate for rainy clouds) and CDNC is cloud droplet number concentration (Feingold and Siebert, 2009). Sorooshian et al. (2009) further estimated S_0 by replacing CDNC with aerosol index (AI). Wang et al. (2012) proposed an alternative metric, the precipitation frequency susceptibility, defined as:

$$S_{POP} = -\frac{d\ln POP}{d\ln AI} \quad (2)$$

where POP is the probability of precipitation. S_{POP} has been shown to strongly correlate with cloud water response to aerosol perturbations in global climate models (Wang et al., 2012;Ghan et al., 2016). Terai et al. (2012； 2015) further extended the definition of precipitation susceptibility:

$$S_X = -\frac{d\ln X}{d\ln CDNC} \quad (3)$$

where X can represent precipitation intensity (I, precipitation rate from rainy clouds only), precipitation fraction (POP, or f) or precipitation rate (R=POP×I, mean precipitation rate from both rainy and non-rainy clouds). Depending on whether I, POP or R is used in Eq. (3), precipitation intensity susceptibility (S_I), precipitation frequency susceptibility (S_{POP} or S_f) or precipitation rate susceptibility (S_R) are therefore defined accordingly. Since R can be decomposed into the product of POP and I, $S_R \approx S_{POP} + S_I$ (Terai et al., 2012, 2015). In addition, some other studies substitute aerosol concentration (N_A) or cloud condensation nuclei (CCN) concentration (N_{CCN}) for CDNC to calculate S_X (Terai et al., 2012; Mann et al., 2014).

The behavior and magnitude of aforementioned precipitation susceptibility metrics varies a lot in different studies. For instance, S_R and S_{POP}, using N_A as an aerosol proxy from Terai et al. (2012), both noticeably decrease with increasing LWP, whereas S_I is flat in the same study. Additionally, previous satellite studies (Wang et al., 2012; Terai et al., 2015; Michibata et al., 2016) show S_X calculated with respect to CDNC is higher than that with respect to AI. The diverse definitions of precipitation susceptibility make it challenging to understand susceptibility discrepancies in different studies. An important objective of this study is to derive these susceptibilities using the same observations in the same context and to better understand their differences through comparisons.

Another source of uncertainty in the estimation of precipitation susceptibility is the uncertainty associated with the observation. Among many others, AMSR-E and MODIS are two widely-used satellite cloud retrieval products in aerosol-cloud interaction studies. For instance, Sorooshian et al. (2009) and Wang et al. (2012) both used AMSR-E LWP

Minghuai Wang 2017/12/5 9:15 PM
已删除: Susceptibility is an quantitative inherent property of the aerosol-cloud system, thereby conveniently comparing this between observation and model estimates.

dell 2017/11/22 3:57 PM
已删除: If it can be estimated based on observations, e.g., satellite remote sensing products, then the impacts of aerosol perturbation can be readily estimated from the product of the susceptibility and the size of the perturbation, e.g., $\Delta A = S_\lambda \Delta CDNC$.

Minghuai Wang 2017/12/5 9:11 AM
已删除: lifetime effects

Minghuai Wang 2017/12/5 9:12 AM
已删除: cloud lifetime effects of

Minghuai Wang 2017/12/5 9:12 AM
已删除: s

product to estimate S_I and S_{POP} with respect to AI, respectively. Terai et al. (2015) and Michibata et al. (2016) used MODIS LWP product to estimate S_I with respect to CDNC. Both products have their advantages and limitations, and are both subject to various retrieval uncertainties. AMSR-E has a coarser spatial resolution than MODIS. Its LWP retrievals are available for both daytime and night time, but suffer from instrument noise, cloud detection issues and beam filling effect (Greenwald et al., 2007; Horváth and Gentemann, 2007; Seethala and Horváth, 2010). MODIS LWP retrievals are available only during daytime. The main uncertainty sources in MODIS LWP retrievals include instrument noise, sub-pixel cloud inhomogeneity, three-dimensional radiative effects and uncertainties in ancillary data (Cho et al., 2015; Platnick et al., 2017; Zhang and Platnick, 2011). A recent study by Seethala and Horváth, (2010) revealed several significant differences between ASMR-E and MODIS LWP products, which could contribute to the aforementioned discrepancy of precipitation susceptibility in the literature.

Additionally, different definitions of rain events and/or different methods to derive rain rates could also lead to discrepancy in observation-based estimation of precipitation susceptibility. For example, the rain rate used in Terai et al. (2015) and Michibata et al. (2016) is simply estimated based on a Z-R relationship from CloudSat radar reflectivity profiles measurements. In contrast, Sorooshian et al. (2009) and Wang et al. (2012) used the rain rate reported in CloudSat operational product, which make use not only radar reflectivity but also path-integrated attenuation in the retrieval process (Haynes et al., 2009). The primary satellite data sets used in the previous studies for estimating precipitation susceptibility are listed in Table. 1. To account for the discrepancy in susceptibility as shown in Table. 1, it's important to examine how different LWP and rain data sets affect the estimates of precipitation susceptibility.

Here we estimate precipitation susceptibility using multi-sensor cloud and aerosol products from A-Train satellites. The main objective of this study is to compare precipitation susceptibility estimates based on different retrieval products, and to better understand discrepancies documented in previous studies. As previous studies have shown that aerosol indirect effect and its uncertainties vary in different cloud dynamical regimes (L'Ecuyer et al., 2009; Wang et al., 2012; Zhang et al., 2016), we further examine how precipitation susceptibility might be different under different atmospheric stability conditions. Section 2 introduces different satellite products and methods used to calculate the susceptibility; Section 3 compares precipitation susceptibility estimates from different satellite products and explores how atmospheric stability affects precipitation susceptibility; finally, the discussions are made in Section 4, followed by the summary in Section 5.

2 Methods

2.1 Satellite datasets

This study mainly uses cloud and aerosol property retrieval products from the Moderate Resolution Imaging Spectroradiometer (MODIS) on Aqua, the Advanced Microwave Scanning Radiometer for Earth Observing System

(AMSR-E) on Aqua, the Cloud Profiling Radar (CPR) on CloudSat and the Cloud-Aerosol Lidar with Orthogonal Polarization (CALIOP) on CALIPSO. All of these satellites operate in the framework of the A-Train constellation (L'Ecuyer and Jiang, 2010; Stephens et al., 2002). Considering most of the warm rainfall occurs in the marine areas (Mülmenstädt et al., 2015) and that satellite retrievals often suffer large uncertainties in the polar regions (Seethala and Horváth, (2010) , the study region is limited to 60°S to 60°N over global oceans, covering the period June 2006 to April 2011. Since MODIS cloud LWP retrieval is only available for daytime, we restrict our analysis to clouds observed in daytime (13:30 local time). MODIS cloud product and CPR radar reflectivity observations used in this study are both provided from the Caltrack datasets, which resample observations from many sensors under CALIOP subtrack with the horizontal resolution of 5km (see the website of http://www.icare.univ-lille1.fr/projects/calxtract/products for more information). For other aerosol and cloud products, including MODIS/CALIOP aerosol products and AMSR-E cloud products, they are further collocated into the CALIOP subtracks in the Caltrack dataset. For each cloud pixel in the Caltrack dataset, the closest aerosol/cloud retrieval sample within one-degree grid box (1°×1°) centered at this Caltrack cloud pixel is chosen. To reduce the uncertainty in cloud retrievals, only samples where MODIS cloud fraction is equal to 100% are selected. The main satellite datasets used in this study are briefly listed in Table. 2.

Minghuai Wang 2017/12/5 10:03 AM
已删除: observations

Minghuai Wang 2017/12/5 10:13 AM
已删除: of collocation between different cloud products,

Minghuai Wang 2017/12/7 9:50 AM
已删除:

Minghuai Wang 2017/12/5 10:16 AM
已删除: Given synergistic observations used in this study, the distance between collocated samples is normally much smaller than 1 degree.

dell 2017/11/16 8:45 AM
已删除: Hence all satellite products have been collocated into the CALIOP tracks with the horizontal resolution of 5 km.

dell 2017/12/8 2:56 PM
已删除: e

Minghuai Wang 2017/12/5 9:27 AM
已删除: To

Minghuai Wang 2017/12/5 9:39 AM
已删除: the potential effect of

Minghuai Wang 2017/12/5 9:39 AM
已删除: on

dell 2017/12/8 2:57 PM
已删除:

Minghuai Wang 2017/12/5 9:27 AM
已删除: , aggregated aerosol grid product is also analyze

dell 2017/12/8 2:57 PM
已删除: d..

2.1.1 AI and CDNC

Three aerosol products are used in the study: MODIS Level 3 daily mean atmosphere product (MYD08_D3, Collection 6), MODIS Level 2 aerosol product (MYD04_L2, Collection 6) and CALIOP Level 2 aerosol layer product (CAL_LID_L2_05kmALay, Version 3.01). The one degree daily mean product of MYD08_D3 is aggregated from MYD04_L2 with 10 km horizontal resolution (Hubanks et al., 2016). This MODIS Level 3 dataset has been used in previous studies to examine aerosol-cloud-precipitation interactions (e.g., L'Ecuyer et al., 2009; Wang et al., 2012) and is compared here with results form the MODIS Level 2 aerosol product to examine how aerosol homogeneity might affect precipitation susceptibility estimates. Horizontal resolution of column aerosol optical depth from CAL_LID_L2_05kmALay product is 5 km. Aerosol property in this dataset is obtained by averaging the 16 aerosol extinction profiles with 333 m of native resolution along track (Young and Vaughan, 2009).

Since AI is a better proxy for CCN concentrations as compared to AOD (Nakajima et al., 2001), AI is calculated as one of the proxy for CCN based on the definition of AI=AOD×AE, where AOD and AE are aerosol optical depth and Ångström coefficient, respectively. For MODIS, AOD at 0.55 μm reported from MYD08_D3 and MYD04_L2 products are based on the Dark Target algorithm over ocean (Kaufman et al., 1997; Tanré et al., 1997; Levy et al., 2013). For CALIOP, AOD at wavelength of 0.532 μm is obtained from the CAL_LID_L2_05kmALay product (Vaughan et al., 2004). Unlike MODIS AE, which is directly reported in aerosol products, AE measurement for CALIOP is calculated based on AOD at 1.064μm and 0.532μm from CAL_LID_L2_05kmALay product (Bréon et al., 2011). Our data screening for CAL_LID_L2_05kmALay

follows a previous study by Kim et al. (2013).

Three aerosol products used in this study are listed in Table 2. It should be noted that all aerosol samples are under cloud free conditions and are selected in close proximity to cloud pixels. Retrievals of aerosol properties from passive sensors and lidar observation are both affected by clouds near the aerosol, and thereby result in overestimation for aerosol property (Chand et al., 2012; Christensen et al., 2017; Tackett and Di Girolamo, 2009). The extent of this overestimation may be different among different sensors, and depends on how far aerosol pixels chosen are from the corresponding cloud pixels (Christensen et al., 2017). This effect, however, would likely impact all metrics in a similar way and we would not expect this effect would impact qualitative comparisons between different metrics.

CDNC is derived from the cloud optical thickness τ and cloud top effective radius r_{eff}, both reported in the MODIS level 2 cloud product (namely, MYD06_L2), based on the following formula (Bennartz, 2007; Quaas et al., 2006):

$$CDNC = \alpha \tau^{0.5} r_{eff}^{-2.5} \quad (4)$$

where the coefficient $\alpha = 1.37 \times 10^{-5} m^{-0.5}$ is estimated based on the assumption that cloud vertical structure follows the classic adiabatic growth model (Quaas et al., 2006). To reduce the uncertainty when deriving CDNC, cloud pixels (identified by Caltrack-MODIS cloud product with the horizontal resolution of 5 km) where cloud optical depth is less than 3 and cloud fraction is less than 100% are excluded (Cho et al., 2015; Zhang and Platnick, 2011). Additionally, we limit our analysis to warm clouds by screening cloud pixels with cloud top temperature warmer than 273K. Under these screening criteria, our results show that 94% warm clouds are single layered (93% in Kubar et al., 2009). Therefore, our analysis mainly focuses on single-layer clouds.

2.1.2 LWP

Cloud LWP for MODIS is diagnosed from solar reflectance observations of r_{eff} and τ as (Platnick et al., 2003):

$$LWP = a \rho_w \tau r_{eff} \quad (5)$$

where ρ_w denotes the liquid water density and a is a constant determined by the assumed vertical variation in cloud droplet size (Greenwald, 2009). For a vertically homogeneous cloud, a = 2/3 (Bennartz, 2007), and a = 5/9 when the adiabatic assumption is applied (Szczodrak et al., 2001). A recent study by Miller et al. (2016) provides a systematic investigation of the impacts of cloud vertical structure on MODIS LWP retrievals. To be consistent with the adiabatic assumption used in Eq. (4) for estimating CDNC, a = 5/9 is applied here.

The other LWP retrieval comes from AMSR-E Level 2B Global Swath Ocean Product (Wentz and Meissner, 2004). Unlike retrieving from solar reflectance of visible near-infrared (VNIR) for MODIS, LWP for AMSR-E is directly derived from brightness temperatures based on liquid-sensitive 37 GHz channel measurements (Seethala and Horváth, 2010). More information of retrieval technique of AMSR-E LWP is documented in Wentz and Meissner (2000). Horizontal resolution of

Minghuai Wang 2017/12/7 9:52 AM
已删除: the

Minghuai Wang 2017/12/7 9:52 AM
已删除: s

Minghuai Wang 2017/12/5 10:39 AM
已删除: .

dell 2017/11/16 10:33 AM
已删除: in clouds

dell 2017/12/8 3:14 PM
已删除: the

Minghuai Wang 2017/12/5 11:40 AM
已删除: (

Minghuai Wang 2017/12/5 11:40 AM
已删除: found that most (93%) of warm clouds are single layered. We also find a similar proportion (94%) of single layer in our dataset by using "Cloud_Multi_Layer_Flag" from MYD06 L2 product.

AMSR-E LWP product (12km) is also different from MODIS LWP product (5km).

2.1.3 Precipitation

Precipitation datasets used in this study are derived from three different products from the CloudSat CPR, namely 2B-GEOPROF, 2C-PRECIP-COLUMN and 2C-RAIN-PROFILE. All the estimates are limited to cloudy profiles by using 2B-GEOPROF cloud mask, which is set to greater than 20 (King et al., 2015). For the 2B-GEOPROF product (Marchand et al., 2008), the maximum radar reflectivity for each cloudy profile is used to define rain event and to estimate rain rate. More specifically, rain rate is obtained by employing the reflectivity-rainfall (Z-R) relationship at cloud base ($Z=25R^{1.3}$ from Comstock et al., 2004), and a radar reflectivity threshold is used to distinguish between drizzling and nondrizzling clouds (Terai et al., 2012, 2015).

The empirical Z-R relationship, however, does not account for multiple-scattering by raindrops and attenuation due to both gases and hydrometeors, which poses major challenges for calculation of rain rate, especially surface rain rate (Lebsock and L'Ecuyer, 2011). To address those challenges, Haynes et al. (2009) introduced a full rainfall retrieval algorithm, which is the basis of the 2C-PRECIP-COLUMN product. The algorithm first makes use of path-integrated attenuation (PIA) derived from measurements of radar backscatter over ocean surface in conjunction with surface wind speed and sea surface temperature. Surface rain rate is then estimated based on a simple algorithm using the PIA. For the 2C-PRECIP-COLUMN product, rain event is identified by using rain likelihood mask. Here, we use flag of "rain certain" to define rain event, which means attenuation-corrected reflectivity near surface is above 0dBZ (Haynes et al., 2009).

2C-PRECIP-COLUMN assumes a constant vertical rain profile in the precipitating column (Haynes et al., 2009), which may not be suitable for warm rain where vertical variation of rain profile is significant (Lebsock and L'Ecuyer, 2011). To address this issue, CloudSat developed a third rain product, 2C-RAIN-PROFILE that utilizes the complete vertically-resolved reflectivity profile observed by the CPR and incorporates a subcloud evaporation model. 2C-RAIN-PROFILE also uses MODIS cloud visible properties to constrain cloud water in its retrieval algorithm (Lebsock and L'Ecuyer, 2011). Note that the 2C-RAIN-PROFILE algorithm directly uses the precipitation occurrence flag from 2C-PRECIP-COLUMN, to define rain events. Thus the probability of precipitation (POP) is the same for both rain products. Note that surface rain rates are only retrieved for those pixels that identified as rain certain in 2C-RAIN-PROFILE product (Lebsock and L'Ecuyer, 2011). Overall, three rain rate datasets in this study are significantly different: rain rate directly estimated from 2B-GEOPROF represents the maximum rainfall rate, precipitation from 2C-PRECIP-COLUMN is the column-mean rainfall rate, and rain rate from 2C-RAIN-PROFILE stands for surface rainfall rate.

2.2 Meteorological datasets

Aerosol-cloud-precipitation interactions and precipitation susceptibility have been shown to depend on cloud regimes

(L'Ecuyer et al., 2009). Following Klein and Hartmann. (1993), we use the lower-tropospheric static stability (LTSS), which is defined as the difference in potential temperature between 700hPa and the surface, to separate different atmosphere thermodynamic regimes. In this study, unstable and stable environments are defined as LTSS less than 13.5K and LTSS larger than 18K, respectively. Pixels where LTSS between 13.5K and 18K are defined as the mid-stable environment (Wang et al., 2012). The European Centre for Medium-Range Weather Forecasts Auxiliary (ECMWF-AUX) product, as an ancillary CloudSat product that contains temperature and pressure within each CPR bin, is used to calculate LTSS.

2.3 Precipitation susceptibility calculation

Following previous studies (Feingold and Siebert, 2009; Sorooshian et al., 2009; Wang et al., 2012; Terai et al., 2012, 2015), precipitation susceptibility is generally defined as:

$$S_{X\_Y} = -\frac{d\ln X}{d\ln Y} \quad (6)$$

where X can be substituted by POP (precipitation frequency), I (precipitation intensity), or R (R=POP×I, precipitation rate), and Y indicates AI or CDNC. Consequently, six different precipitation susceptibilities can be obtained from the observations described above. To constrain cloud macrophysical environment, all samples are sorted according to their LWP values first and then divided into 10 LWP bins. The ratio of the number of pixels in each bin to the total pixels ranges from 5% to 14%. For each LWP bin, samples are sorted by AI or CDNC, and ten AI/CDNC bins are equally divided to calculate POP, mean I, R, AI and CDNC within each AI/CDNC bin. Finally, the values of S_{X_Y} are derived by linear regression in log-log space.

3 Results

3.1 S_{X_AI} versus S_{X_CDNC}

S_{X_AI} and S_{X_CDNC} as a function of LWP are shown in Fig. 1. Here LWP from MODIS and rain data from 2B-GEOPROF with a rain threshold of -15dBZ are used, to better compare with other satellite studies (Terai et al., 2015; Michibata et al., 2016). Here AI is estimated by using MYD04 dataset and detailed comparison among different aerosol products will be discussed in Section 3.2.

Consistent with previous studies, S_{X_AI} are generally much smaller than S_{X_CDNC} as shown in Fig. 1. S_{POP_AI} from Wang et al. (2012) is less than 0.2 over all LWP bins, while Terai et al. (2015) showed that S_{POP_CDNC} decreases with increasing LWP, ranging from 1 to 0, and S_{R_CDNC} is maintained at around 0.5. Fig. 1b further shows S_{I_CDNC} monotonically increases with LWP, followed by a slight decrease. Although the S_{I_CDNC} peak (around 0.6 with LWP 350 gm^{-2}) is not significant in Fig. 1b, S_{I_CDNC} would decrease distinctly after the peak if the upper bound of LWP and the number of LWP bins both increase (not shown). This turning point may correspond to conversion process shifting from the autoconversion to accretion regime (Michibata et al., 2016).

dell 2017/11/14 4:01 PM
已删除: cloud

Minghuai Wang 2017/12/7 4:47 PM
已删除: higher

Minghuai Wang 2017/12/7 4:47 PM
已删除: s

Minghuai Wang 2017/12/7 4:48 PM
已删除: is relatively small, there are still more than ten thousand pixels for those LWP bins.

dell 2017/11/23 8:09 PM
已删除: T

Minghuai Wang 2017/12/7 11:26 PM
已删除: ary

Minghuai Wang 2017/12/7 11:26 PM
已删除: ed

dell 2017/11/23 8:22 PM
已删除: around 0.6 with LWP 400 gm^{-2}, is in good agreement with result of Michibata et al. (2016), which suggested that the turning point corresponds to

To account for discrepancy between S_{X_AI} and S_{X_CDNC}, we use the condition probability method (Gryspeerdt et al., 2016) to explore relationships between AI and CDNC. As Fig. 2a shows, the majority of CDNC values concentrate on the intervals between 20 cm^{-3} to 100 cm^{-3}, representing an upward tendency with increasing AI over global oceans. The similar feature of CDNC with AI is also shown in different LTSS conditions (Fig. 2b, 2c and 2d). Note that fluctuation of the curve at high AI results from the small number of effective pixels, especially in unstable condition.

To formally account for the relationship between CDNC and AI, S_{X_AI} can be decomposed into two parts:

$$S_{X\_AI} = -\frac{d\ln X}{d\ln AI} = -\frac{d\ln X}{d\ln CDNC}\frac{d\ln CDNC}{d\ln AI} = S_{X\_CDNC}\frac{d\ln CDNC}{d\ln AI} \quad (7)$$

where dlnCDNC/dlnAI is the link between S_{X_AI} and S_{X_CDNC}. S_{X_AI} is expected to be smaller than S_{X_CDNC} if dlnCDNC/dlnAI is smaller than 1. Fig. 3 shows dlnCDNC/dlnAI over global oceans, which is calculated by log-log linear regressions in each MODIS LWP bin. dlnCDNC/dlnAI is smaller than 0.4, which explains why S_{X_AI} is generally smaller than S_{X_CDNC}. Table 3 further shows the LWP-weighted mean of dlnCDNC/dlnAI, S_{X_AI}, and S_{X_CDNC} over global oceans. Our results are consistent with the previous satellite observations. For instance, S_{POP_AI} is equal to 0.11 in our results obtained from AMSR-E LWP, close to the value of 0.12 in Wang et al. (2012), and our S_{R_CDNC} derived from MODIS LWP is 0.74, similar to that (0.6) in Terai et al. (2015). Since the global mean dlnCDNC/dlnAI is about 0.3, we would expect S_{X_AI} is about one-third of S_{X_CDNC}, according to Eq. (7). Table 3 shows that this relationship is generally true for S_{POP}, but less so for S_I, especially for S_I calculated based on MODIS LWP.

Table 3 further demonstrates that $S_R \approx S_I + S_{POP}$ is generally true for different LWP products and over different stability regimes, consistent with Terai et al. (2015).

3.2 S_{X_AI} from different aerosol products

Now we explore how precipitation susceptibility estimates might be different from different aerosol products (i.e., MYD04, MYD08 and CAL_LID_L2_05kmALay). As shown in Figure 4, despite differences in their horizontal resolutions (10 km versus 1 degree), S_{X_AI} calculated from MYD04 and MYD08 agrees well (Fig. 4a and Fig. 4b), which may result from the fact that aerosol layers are likely homogeneous over relatively large spatial scales less than 200 km (Anderson et al., 2003), especially over global oceans. In addition, McComiskey and Feingold (2012) found that the statistics (i.e., min, max and variance) of AOD are constant between MYD04 and MYD08 products over the northeast Pacific Ocean for a given day. Although not shown here, the probability distributions of AI derived from MYD04 and MYD08 products are qualitatively similar over global oceans. In comparison with the results based on MODIS retrievals, S_{X_AI} obtained from CALIOP (Fig. 4c) is smaller and relatively flat across all LWP bins. Further test shows that S_{X_AI} using CALIOP AOD but MYD04 AE agrees better with that based on MODIS aerosol products (Fig. 4d). This suggests that differences in AE estimates from MODIS and CALIOP largely explain the discrepancy between two aerosol products. Previous studies indicate that MODIS and CALIOP AOD are poorly correlated (e.g., Costantino and Bréon, 2010; Kim et al., 2013; Kittaka et al., 2011; Ma et al.,

2013). Our results suggest that differences in AOD retrievals can lead to differences in AE estimates and further affect AI and precipitation susceptibly estimates. Given that AI from MODIS has been widely used in previous studies for examining aerosol-cloud-precipitation interactions, for the rest of the paper, AI from MYD04 is used, unless otherwise stated.

3.3 S_{X_Y} from different LWP dataset

Figure 5 shows the behavior of S_{POP} and S_I based on different LWP data sets (i.e., AMSR-E and MODIS LWP). Estimates of rain rate and rain events are based on 2B-GEOPROF with -15dBZ threshold as mentioned in Section 2.1.3. Here we focus on characteristics of S_{POP} and S_I since $S_R \approx S_I + S_{POP}$ as mentioned in Section 3.1. As shown in Fig. 5a, S_{POP_CDNC} based on MODIS LWP is similar to that calculated based on AMSR-E LWP. This consistency is also found for S_{POP_AI}. In contrast, S_{I_CDNC} and S_{I_AI} calculated based on two LWP products are quite different (Fig. 5b). S_{I_CDNC} based on MODIS LWP are significantly larger than that based on AMSR-E LWP over all LWP bins (see upward triangles in Fig. 5b), while S_{I_AI} from two LWP products shows an opposite pattern: S_{I_AI} based on MODIS LWP is lower than that based on AMSR-E LWP (see downward triangles in Fig. 5b). These features of discrepancies in S_I between MODIS and AMSR-E LWP are still applicable to S_{POP}, though the magnitude is much smaller and is not statistically significant (Fig. 5a).

Fig. 5b shows that LWP value where S_{I_CDNC} peaks based on MODIS LWP is larger than that based on AMSR-E LWP. Large eddy simulation analysis by Duong et al. (2011) showed a similar shift in LWP with changing spatial resolutions, which is attributed to reduction in mean LWP at coarser resolutions. However, Fig. 6 shows that there is no systematic shift in the frequency distribution of LWP between two LWP products, regardless of precipitation or non-precipitation samples.

To better understand the discrepancy in precipitation susceptibility estimates from two LWP products in Fig. 5, we plot POP and intensity as a function of CDNC/AI in log space for each LWP bin obtained from MODIS and AMSR-E. Fig. 7a-7d shows that the relationships between POP and CDNC (AI) from MODIS LWP are similar to that from AMSR-E LWP. In contrast, intensity versus CDNC (AI) between two LWP products shows large differences (Fig. 7e-7h). Fig. 7f shows that intensity is positively correlated with CDNC at low CDNC for high AMSR-E LWP bins, which helps to explain why S_{I_CDNC} from AMSR-E LWP is smaller than that from MODIS, especially at high LWP bins (Fig. 5b).

Combining Eq. (4) and (5), CDNC from MODIS can be reformulated as a function of LWP and r_{eff}:

$$CDNC = \alpha (a\rho_w)^{-0.5} LWP^{0.5} r_{eff}^{-3} \quad (8)$$

where α, a and ρ_w are all constant. Accordingly, r_{eff} decreases with increasing CDNC for any given MODIS LWP bin, and larger CDNC leads to smaller r_{eff}, which further results in reduction in precipitation efficiency, as shown in Fig. 7e. The CDNC-r_{eff} relationship still holds when data is binned by AMSR-E LWP and r_{eff} decreases with increasing CDNC even at larger LWP AMSRE-LWP bins (Fig. 8a). We would then expect rain intensity still decreases with increasing CDNC for the AMSR-E LWP at low CDNC. So then what might lead to increases in precipitation intensity with increasing CDNC at low

Minghuai Wang 2017/12/7 4:58 PM
已删除: F

dell 2017/11/28 3:19 PM
已删除: squares

dell 2017/11/28 3:20 PM
已删除: points

Minghuai Wang 2017/12/5 10:00 PM
已删除: the discrepancies

Minghuai Wang 2017/12/5 10:00 PM
已删除: are

Minghuai Wang 2017/12/7 5:02 PM
已删除: significant

CDNC when data are binned according to constant AMSR-E LWP (Fig. 7f)? Our analysis suggests that this might come from the discrepancies in two LWP products under low CDNC. Fig. 8b shows that, under constant AMSR-E LWP, MODIS LWP significantly varies with CDNC (Fig. 8b). In particular, MODIS LWP rapidly increases with CDNC at low CDNC, which might explain why rain intensity increases with increasing CDNC at low CDNC under constant AMSR-E LWP, which further leads to much smaller S_{I_CDNC} from AMSR-E LWP. Our results further indicate that rain intensity retrieval from CloudSat might be more consistent with LWP retrieval from MODIS than that from AMSR-E, as under constant AMSR-E LWP, rain intensity increases with increasing MODIS LWP at low CDNC (Fig. 7f and Fig. 8b).

It is interesting to note that, for rainy pixels, difference in LWP between MODIS and AMSR-E varies with MODIS CDNC. Under constant AMSR-E LWP (larger than 200 g m^{-2}), MODIS LWP dramatically increases with increasing CDNC at lower CDNC (< ~25 cm^{-3}). These features are also applicable to non-rainy samples (not shown). Further studies are needed to understand the aforementioned discrepancy.

3.4 S_{X_Y} from different rainfall definition

Given that rainy samples may be dominated by different precipitation process (e.g., autoconversion vs. accretion process) with increasing threshold for defining a rainfall event (Jung et al., 2016), precipitation susceptibility may be changed when we apply different rainfall thresholds. To examine this, we plot S_{POP} and S_I under different thresholds (i.e., -15dBZ and 0dBZ of maximum radar reflectivity) used to define a rain event based on 2B-GEOPROF products. These thresholds of -15dBZ and 0dBZ correspond to approximately precipitation rate of 0.14 and 2 mm d^{-1}, respectively (Comstock et al., 2004). Hence, precipitation susceptibilities under these two thresholds can be referred to as drizzle (> -15 dBZ) and rain (> 0 dBZ) susceptibilities. As Fig. 9 indicates, difference in S_{X_AI} between drizzle and rain is, at first glance, less evident compared to S_{X_CDNC}. This can be partly attributed to the low values of S_{X_AI} themselves. Relative differences in S_{X_AI} are even larger than that of S_{X_CDNC} at low AMSR-E LWP (not shown). Fig. 9a and Fig. 9c show that rain S_{POP_AI} is higher than that of drizzle over most LWP bins, which is consistent with results from Wang et al. (2012).

Rainfall definition significantly impacts S_{POP_CDNC} and S_{I_CDNC}: increasing the threshold results in reduction of S_{I_CDNC} over all LWP and, by contrast, leads to distinctly increase in S_{POP_CDNC}, especially at moderate LWP (see Fig. 9). These overall changes in S_{I_CDNC} and S_{POP_CDNC} after increasing the threshold are consistent with Terai et al. (2015). The observational result from Mann et al. (2014) have also shown an evident increase in S_{POP} with respect to N_{CCN} at high LWP with increasing thresholds. The systematic increase in S_{POP_CDNC} may result from larger proportion of non-drizzling samples with increasing threshold. The reduction of S_{I_CDNC} is in agreement with previous studies (Duong et al., 2011; Jung et al., 2016). Although not shown here, for a fixed threshold, there is no significant discrepancy between the results of S_{I_CDNC} and S_{R_CDNC} based on different Z-R relationships ($Z=25R^{1.3}$ and $Z=302R^{0.9}$ are used both from Comstock et al. 2004, which aim at cloud base and surface rain rate, respectively), which is consistent with the result from Terai et al. (2012).

dell 2017/11/16 10:49 AM
已删除: is

Minghuai Wang 2017/12/7 5:05 PM
已删除: help to

dell 2017/11/30 9:40 AM
已删除: _CDNC

Overall, our results show that S_{POP} and S_I are both sensitive to the rainfall definition and that S_{POP} is greater for rain while S_I is greater for drizzle. Our results further imply that onset of drizzle is not as readily suppressed in warm clouds as rainfall (i.e., S_{POP} is greater for rain than for drizzle). By contrast, S_R is not affected by the rainfall definition since the mean rain rate R for a given LWP/CDNC or LWP/AI bin is calculated based on both rainy and non-rainy clouds and does not depend on rainfall thresholds (not shown).

While the response of precipitation susceptibility to change in threshold shows the same pattern between MODIS and AMSR-E LWP (Fig. 9), the extent to which susceptibility changes with increasing threshold is quite different between these LWP products. Overall, sensitivity of S_{X_CDNC} to different thresholds using MODIS LWP is larger than that based on AMSR-E LWP; this pattern is opposite for S_{X_AI}. It is interesting to note that while the difference in S_{POP} between MODIS and AMSR-E LWP is small with the -15dBZ threshold (Fig. 5; Fig. 9a and Fig. 9c), the difference is relatively larger for the 0 dBZ threshold (Fig. 9a and Fig. 9c), especially at larger LWP bins.

3.5 S_{X_Y} from different precipitation data sets

The diverse rain data sets allow us to explore differences in precipitation susceptibility estimates from different rain products. In Fig. 10, we illustrate S_{POP} and S_I for different rain data sets, namely, 2B-GEOPROF, 2C-PRECIP-COLUMN and 2C-RAIN-PROFILE (Marchand et al., 2008; Haynes et al., 2009; Lebsock and L'Ecuyer, 2011) products. Here we use LWP derived from MODIS and use "rain certain" flag for rain definition reported in the latter two rain products. Since the precipitation flags used in these two rain products are identical (Lebsock and L'Ecuyer, 2011), only S_{POP} based on 2C-PRECIP-COLUMN is plotted in Fig. 10. For 2B-GEOPROF, the threshold of 0dBZ radar reflectivity is used to define a rain event and rain rate is estimated by using $Z=25R^{1.3}$ suggested by Comstock et al. (2004). Note that using "rain certain" flag or threshold of 0 dBZ to identify rain event for those rain products would result in a reduction of rain events across all LWP bins, especially at low LWP bins, therefore we expand bounds of low LWP bins to include enough rain samples at low LWP bins.

S_{POP} exhibits a similar dependence on LWP among these three rain products, but S_{POP} based on 2B-GEOPROF is systematically larger than that based on 2C-PRECIP-COLUMN (this is also true for S_I). It is unclear what might lead to higher S_{POP} and S_I from 2B-GEOPROF. The vertical structure of clouds may play a role here, as the maximum radar reflectivity is used from 2B-GEOPROF and surface rain rates are used from the other products.

The most significant discrepancy occurs in S_{I_CDNC} and S_{I_AI} (see Fig. 10b). Fig. 10b shows that S_{I_CDNC} and S_{I_AI} are both near-zero for LWP <400 g m^{-2}, which may be attributed to high thresholds used among the three rain products. This indicates that precipitation intensity with high threshold is insensitive to CDNC and AI at moderate LWP. This result is consistent with Terai et al. (2015) who suggested that heavy drizzle intensity is insensitive to CDNC. As Fig. 10b shows, S_{I_CDNC} based on 2C-RAIN-PROFILE product (red squares in Fig. 10b) with subcloud evaporation model incorporated is

Minghuai Wang 2017/12/5 10:17 PM
已删除: mean

Minghuai Wang 2017/12/5 10:18 PM
已删除: rain

Minghuai Wang 2017/12/5 10:18 PM
已删除: of

Minghuai Wang 2017/12/5 10:19 PM
已删除: any given LWP/CDNC or LWP/AI bin would not change if

Minghuai Wang 2017/12/5 10:19 PM
已删除:

Minghuai Wang 2017/12/7 11:28 PM
已删除: changes

dell 2017/11/29 7:43 PM
已删除: more significant

Minghuai Wang 2017/12/7 5:13 PM
已删除: exactly

Minghuai Wang 2017/12/7 5:14 PM
已删除: have

higher than that based on 2C-PRECIP-COLUMN product (blue squares in Fig. 10b) at high LWP (above 300 gm^{-2}). Hill et al. (2015) showed that, when considering rain evaporation, S_{I_CDNC} based on surface rain rate is larger than that based on cloud base and column max rain rate at LWP > 400 gm^{-2}. However, their difference is more obvious than our results, which may result from threshold used (0.01 mm day^{-1} in Hill et al. (2015) versus surface the 0 dBZ in 2C-RAIN-PROFILE and 2C-PRECIP-COLUMN products). It is interesting to note that the sign of S_{I_CDNC} at large LWP is different from that of S_{I_AI} (Fig. 10b), which is not true for AMSR-E LWP (not shown). This warrants further investigation in the future.

dell 2017/11/16 10:46 AM
已删除: h

3.6 S_{X_Y} under different stability regimes

Here we examine precipitation susceptibility under different atmospheric stability regimes, as aerosol-cloud-precipitation interactions have been shown to differ under different stability regimes (e.g., L'Ecuyer et al., 2009; Zhang et al., 2016; Michibata et al., 2016). Based on MODIS LWP and 2B-GEOPROF product with -15 dBZ threshold, Fig. 11a and Fig. 11b suggest that both S_{POP} and S_I increase with more stable environment. This pattern for S_{POP} is consistent with the findings of L'Ecuyer et al. (2009) who showed that suppression of precipitation was largest at lower LWP in stable environments. Terai et al. (2015) also found maximum S_{POP_CDNC} occurred in regions where stable regime was predominant. The distribution of the precipitation susceptibility with respect to LTSS and LWP shown in Fig. 12 using 2B-GEOPROF product with the -15 dBZ rain threshold is consistent with Fig. 11a and Fig. 11b: S_{POP} increases with increasing LTSS with the exception of high LWP. Although not shown here, S_{POP_AI} based on 2C-PRECIP-COLUMN and AMSR-E LWP product produces a similar pattern with the result of L'Ecuyer et al. (2009), who showed the slope between POP and AI is small both at low and high LWP, but this magnitude tends to increase at intermediate LWP and high LTSS.

Minghuai Wang 2017/12/7 5:29 PM
已删除: be different

Minghuai Wang 2017/12/7 5:30 PM
已删除: vides

Rain definition significantly affects spread of S_{POP} and S_I under different stability regimes. As rain threshold increases, the discrepancy in S_{POP} among different LTSS conditions is more significant (Fig. 11c versus Fig. 11a) while discrepancy in S_I becomes smaller. LTSS-dependence of S_I is even reversed at low LWP with the 0 dBZ threshold compared to that using the -15 dBZ threshold (Fig. 11d versus Fig. 11b).

The above-mentioned features of LTSS-dependency are also true in terms of LWP-weighed mean value, as shown in Fig. 13. For all those cases based on different rain products and LWP products, the LWP-weighed mean of S_{POP} is generally larger under stable conditions compared with unstable conditions. Yet, this feature does not hold true for S_I except the case based on the 2B-GEOPROF dataset with the -15 dBZ threshold. Our results also suggest that it is important to account for the influence of atmospheric stability owing to the clear dependence of S_{POP} on metrics like LTSS, though it is acknowledged that LTSS alone is an imperfect metric for isolating cloud regimes (e.g., Nam and Quaas, 2013). Different metrics associated with cloud regimes should be examined in future to better understand the effect of cloud regimes on precipitation susceptibility. For instance, LTSS can be combined with vertical pressure velocity to distinguish between different cloud types (Zhang et al., 2016).

Minghuai Wang 2017/12/9 8:28 PM
已设置格式: 字体:10 pt

Minghuai Wang 2017/12/9 8:28 PM
已设置格式: 字体:10 pt

Minghuai Wang 2017/12/9 8:29 PM
已删除: Note that LTSS alone may be insufficient for distinction betweencloud regimes (Nam and Quaas, 2013), therefore,

Minghuai Wang 2017/12/5 3:51 PM
已删除: d

4 Discussion

Fig. 14 shows the range of precipitation susceptibility estimated from different LWP and rain products. Here the threshold of 0dBZ of maximum radar reflectivity is used for 2B-GEOPROF product and the "rain certain" flag is used for 2C-PRECIP-COLUMN and 2C-RAIN-PROFILE products. It shows that uncertainties in S_{POP} (Fig. 14a) as a result of using different LWP and/or rain products are smaller than the uncertainties associated with S_I and S_R (Fig. 14b and c). The uncertainties in S_{POP} are mainly attributed to different LWP products as described in Section 3.4 (see red symbols in Fig. 9a and Fig. 9c).

Our results may help to reconcile some of the differences in previous estimates of precipitation susceptibility. For example, our results show that $S_{X\_AI} \approx 0.3 S_{X\_CDNC}$ (Table 3 and Fig. 1), which explains why S_{POP_CDNC} in Terai et al. (2015) is much larger than S_{POP_AI} in Wang et al., (2012). Previous studies are also different in how precipitation susceptibility varies with increasing LWP. Our results show that S_I generally increases with LWP at low and moderate LWP and then decreases with increasing LWP at moderate and high LWP, consistent with results from Feingold et al., (2013), Michibata et al., (2016) and Jung et al., (2016). The monotonic increase of S_{I_CDNC} with increasing LWP in Terai et al., (2015) is mainly because that the LWP range in their study is relatively narrow (from 0 to ~400 g m^{-2}) and our results suggest that when the upper bound of LWP is extended to ~800 g m^{-2}, the "descending branch" (S decreases with increasing LWP) noted in Feingold et al. (2013) appears, though the exact LWP value where S_{I_CDNC} peaks depend on LWP and rain products used as well as the rainfall threshold choices.

Interestingly, S_I tends to be negative at low LWP both for AMSR-E and MODIS LWP (Fig. 5b). This is closely associated with positive correlation between conditional-mean rainfall intensity and CDNC (AI) at low LWP bins where CDNC (AI) is high (Fig. 7e-7h). More negative values are captured when S_I is estimated using 2C-PRECIP-COLUMN and 2C-RAIN-PROFILE products and using high rainfall thresholds (Fig. 9b, Fig. 9d, Fig. 10b and Fig. 13). Furthermore, based on these rain products, S_{I_CDNC} is all negative at low and intermediate LWP regardless of the LWP dataset used (Fig. 10b) and almost all of mean S_{I_CDNC} is significantly negative regardless of stability regimes (Fig. 13). Depending on LWP products adopted, using AI instead of CDNC in estimating S_I can make it less negative (for AMSR-E LWP) or more negative (for MODIS LWP) (Fig. 13). Terai et al. (2015) also found negative values of S_{I_CDNC} at low LWP and high CDNC. In their study, sign and/or magnitude of S_{I_CDNC} at low LWP are distinct across different regions. In addition, Koren et al. (2014) found a positive relationship between AOD and rain rate over pristine areas with warm and aerosol-limited clouds, which was attributed to aerosol invigoration effect. As S_I shows large differences under different stability regimes (Fig. 13), it would be highly interesting to analyze regional variation in S_I to further understand negative S_I in the future, especially under unstable regimes.

Furthermore, our results show that drizzle intensity is more susceptible to aerosol perturbations than rain intensity (see

Minghuai Wang 2017/12/6 10:17 AM
已删除: The relationship of susceptibility between different metrics (i.e., $S_R \approx S_I + S_{POP}$, $S_{X\_AI} \approx 0.3 S_{X\_CDNC}$) may partly explain the differences in magnitude of susceptibility in precious studies

dell 2017/12/8 4:45 PM
已删除: ,

Minghuai Wang 2017/12/6 10:00 AM
已删除: , e.g.,

Minghuai Wang 2017/12/6 10:19 PM
已删除: ,

Minghuai Wang 2017/12/6 2:13 PM
已删除: h high

Minghuai Wang 2017/12/6 3:54 PM
已删除: In addition, the behavior of susceptibility may be affected by LWP range and LWP bin setting. For instance, our results and Terai et al., (2015) both show that S_{I_CDNC} monotonically increase with LWP increasing (Fig. 1b in current study and Fig. 1c in Terai et al., (2015)), which is inconsistent with the behavior of S_{I_CDNC} from Michibata et al., (2016) with decreasing tread after increasing. However, if we increase both the upper boundary of LWP and the number of LWP bins, S_{I_CDNC} would decrease distinctly after the peak (not shown).The results presented here also show that "the descending branch" (S decreases with increasing LWP) and "the ascending branch" (S increases with increasing LWP) of S_{I_CDNC} noted in Feingold et al. (2013) is not only subject to LWP or rain products (Fig. 145b), but also to thresholds chosen to define a rain event (Fig. 9b and Fig. 9d). Therefore, LWP and rain products themselves play a nonnegligible role when accounting for discrepancy in S_{I_CDNC} in existing studies. In addition, both S_{POP} and S_I are generally sensitive to the rain threshold choice (Fig. 9).

Minghuai Wang 2017/12/7 6:09 PM
已删除: we estimate

dell 2017/12/2 11:11 AM
已删除: based on these rain products

dell 2017/12/8 4:48 PM
已删除:

Fig. 9b and Fig. 9d), which might help to explain why negative values of S_{I_CDNC} occur more frequently with increasing rainfall thresholds. Jung et al. (2016) found more negative values of S_{I_CDNC} with increasing threshold (see Fig. B2 in Jung et al. (2016)). In addition, rain products used in our study are all derived from CPR onboard CloudSat. With increasing thresholds, rainfall becomes heavy and uncertainty in rain rate retrieval can grow as CPR is insensitive to heavy precipitation (Haynes et al., 2009). So combination of different rain satellite products (e.g., CloudSat and TRMM) would be helpful for better understanding negative S_I.

It should be noted that precipitation susceptibility in our study is based on Eq. (7) and is derived by linear regression between precipitation fields and CDNC/AI in log-log space. The negative/positive correlation between precipitation frequency/intensity and aerosols may not be readily explained as aerosol effects on precipitation. For example, a negative correlation between precipitation frequency and aerosols may come from the wet scavenging effects of aerosols (more precipitation leads to less aerosols) but not aerosol suppression of precipitation. However, in our study, we not only calculate precipitation susceptibility with respect to AI (S_{X_AI}), but also with respect to CDNC (S_{X_CDNC}) and the later one is expected to be less affected by the wet scavenging effects. The broad consistency between these two estimates shown in our results (Fig. 13), especially for the estimate of S_{POP}, lends the support to the limited influence of wet scavenging in our estimate. Further support for this comes from the fact that precipitation susceptibility estimates based on the 1 degree L3 MODIS aerosol products are similar to those based on the 10 km L2 MODIS aerosol products (Fig. 4), as we would expect the wet scavenging effects are more important at smaller scales if the wet scavenging effects are a dominating factor. Nevertheless, the effects of wet scavenging can still be important in satellite studies of aerosol-cloud-precipitation interactions, and should be better quantified in future, perhaps in combination with model simulations.

5 Summary

In this paper, we estimate precipitation susceptibility on warm clouds over global oceans based on multi-sensor aerosol and cloud products from the A-Train satellites, including MODIS, AMSR-E, CALIOP and CPR observations, covering the period June 2006 to April 2011. In addition to different aerosol, cloud and rain products, we also analyze other factors that have potential influence on susceptibility, such as different definitions of precipitation susceptibility (six different susceptibilities defined by Eq. (6)), stability regimes, and different thresholds for defining a rain event (i.e., -15dBZ and 0dBZ of maximum radar reflectivity for 2B-GEOPROF). The primary goal of the study is to quantify uncertainties in precipitation susceptibility estimates from satellite observations.

Minghuai Wang 2017/12/7 6:27 PM
已删除: e.g.,

In general, S_{POP} is a relatively robust metric throughout different LWP and rain products and its estimate is less sensitive to different datasets used (Fig. 13-14). S_{POP_CDNC} shows overall a monotonic decreasing trend with respect to LWP. S_{POP_AI} increases to a maximum at low LWP and then decreases with higher LWP. In contrast, S_I differs considerably among

different LWP and rain products (Fig. 13-14). Interestingly, S_{I_CDNC} and S_{I_AI} differ between those LWP products with opposite pattern: S_{I_CDNC} based on MODIS LWP is higher than that using AMSR-E LWP and the reverse is true for S_{I_AI} (Fig. 13). Negative S_I is found in our study, especially at low LWP. However, the extent of negative S_I depends on LWP and rain products, rainfall thresholds, and whether S_I is calculated with respect to AI or CDNC (Fig. 13). More negative values are found when S_I is calculated based on 2C-PRECIP-COLUMN and 2C-RAIN-PROFILE products, and S_I based on rain samples (with 0 dBZ threshold) tends to be more negative. Further studies (regional variation in S_I, combination of different rain satellite products, etc.) are needed to understand this issue.

Precipitation susceptibility for drizzle (with -15 dBZ rainfall threshold) is significantly different from that for rain (with 0 dBZ rainfall threshold) (Fig. 9 and Fig. 13). Our results suggest that onset of drizzle is not as readily suppressed by increases in AI or CDNC in warm clouds as rainfall (i.e., S_{POP} is smaller for drizzle than for rain, especially at moderate LWP, Fig. 9). This may partly come from the fact that POP of drizzle is close to 100% at moderate and high LWP regardless of CDNC or AI values (Fig. 7a-d), which makes it insensitive to perturbations in CDNC or AI and results in smaller S_{POP} at these LWP bins compared with S_{POP} for rain (Fig. 9). On the other hand, precipitation intensity susceptibility is generally smaller for rain than for drizzle. This is consistent with our expectation that when precipitation intensity increases, accretion contributes more to the production of precipitation, which makes precipitation intensity less sensitive to perturbation in CDNC or AI, as accretion is less dependent on CDNC compared with autconversion (Feingold et al., 2013; Wood, 2005). In addition, the extent of these differences between drizzle and rain depends on the LWP products used.

S_{X_AI} based on aerosol products at different spatial resolutions (i.e., 10 km versus 1 degree) is consistent with each other. Chen et al. (2014) also found that aerosol indirect forcing derived from satellite observations was similar from AI observations at different resolutions (i.e., 20 km versus 1 degree). This suggests that aerosol layers over oceans are relatively homogeneous, implying that aerosol properties at coarse resolution may be suitable for studying aerosol-cloud interactions over oceans.

S_{POP} strongly depends on LTSS, with larger values under more stable environment. This dependence is evident over all LWP bins, especially at low and moderate LWP bins and is more significant for rain than for drizzle (Fig. 11 and Fig. 13). These features, however, are less robust for S_I throughout different LWP and rain products as S_I estimates show large uncertainties from different datasets (Fig. 13). Only in the case of S_I estimated from 2B-GEOPROF product for drizzle (with -15 dBZ threshold), does the LTSS-dependence of S_I hold for both MODIS and AMSR-E LWP. The pattern of S_{POP_AI} under different stability conditions from our paper (Fig. 13b and Fig. 13f) is consistent with the findings of L'Ecuyer et al., (2009). In addition, Terai et al., (2015) found maximum S_{POP_CDNC} occurred in regions where stable regime is predominant. Lebo and Feingold (2014) calculated precipitation susceptibility for stratocumulus and trade wind cumulus using large-eddy simulations (LES) and included an overview of precipitation susceptibility estimates based on LES in the literature. However, their results focus on the relationship between precipitation susceptibility and cloud water response to aerosol perturbations,

Minghuai Wang 2017/12/7 6:39 PM
已删除: It is interesting to note that S_I is negative at low LWP.

Minghuai Wang 2017/12/7 6:39 PM
已删除: . Our results show that these negative values of S_I may be related to stability regimes and further show that

Minghuai Wang 2017/12/7 9:33 PM
已删除:

Minghuai Wang 2017/12/6 8:25 AM
已删除: significant

Minghuai Wang 2017/12/6 8:25 AM
已删除: larg

Minghuai Wang 2017/12/6 8:26 AM
已删除: rain

Minghuai Wang 2017/12/6 8:26 AM
已删除: drizzle

Minghuai Wang 2017/12/6 8:22 AM
已删除: Given that drizzle

Minghuai Wang 2017/12/6 8:24 AM
已删除: maintains almost

Minghuai Wang 2017/12/6 8:30 AM
已删除: the increase in rain S_{POP} may be related to larger proportion of non-rain samples with increasing threshold (not shown), and thereby possible change in rain POP with CDNC or AI at moderate and high LWP.

Minghuai Wang 2017/12/6 8:40 AM
已删除: And this decrease mainly result from that rain samples with higher intensity, which are more strongly dependent on accretion process, are more independent on CDNC

and did not examine how precipitation susceptibility might be different for clouds under different cloud regimes. The physical mechansims behind the strong dependence of S_{POP} on stability are still unclear and warrant further investigation in the future.

The results presented here show that the discrepancy in magnitude between S_{X_AI} and S_{X_CDNC} can be mainly attributed to the dependency of CDNC on AI. On the global scale, our results show that S_{X_AI} is about one-third of S_{X_CDNC}. This relationship is more applicable to S_{POP}, and is less applicable to S_I. In addition, $S_R \approx S_I + S_{POP}$ is generally true for different LWP products and over different LTSS conditions.

As S_{POP} demonstrates relatively robust features across different LWP and rain products, this makes it a valuable metric for quantifying aerosol-cloud-precipitation interactions in observations and models. For instance, it would be highly interesting to examine why S_{POP} strongly depends on atmospheric stability and how well this dependence is represented in a hierarchy of models (e.g., large eddy simulations, cloud resolving models, regional climate models, and global climate models). We also note that $S_{POP\ CDNC}$ is generally less uncertain compared to $S_{POP\ AI}$ and that a relatively robust relationship between $S_{POP\ CDNC}$ and $S_{POP\ AI}$ exists (i.e., $S_{X\_AI} \approx 0.3 S_{X\_CDNC}$) (Fig. 13 and Table 3). Given that aerosol retrievals near clouds are still challenging and aerosol-cloud relationships in satellite observations can be affected by aerosol retrieval contaminations from clouds, we recommend to first thoroughly quantify $S_{POP\ CDNC}$ in observations and models. As $S_{POP\ CDNC}$ is derived based on CDNC instead of AI, $S_{POP\ CDNC}$ is also not influenced by wet scavenging. Only after $S_{POP\ CDNC}$ is thoroughly quantified, we can then combine it with how CDNC depends on AI to better quantify $S_{POP\ AI}$.

On the other hand, S_I estimates strongly depend on satellite retrieval products. Uncertainties in S_I estimate are particular large when S_I is estimated based on rain samples (> 0 dBZ) rather than drizzle samples (> -15 dBZ). It would then be desirable to use drizzle samples to estimate S_I. However, satellite retrieval of precipitation rate for drizzle can be highly uncertain. It is therefore recommended to further improve the retrieval accuracy of precipitation rate for drizzle in satellite observations in order to better use satellite estimate of S_I to quantify aerosol-cloud precipitation interactions. Alternatively, long-term ground and in-situ observations with high accuracy precipitation rate retrievals can be used to provide better estimate S_I and to further quantify aerosol-cloud-precipitation interactions.

dell 2017/12/8 9:41 AM
已删除:

Minghuai Wang 2017/12/7 9:50 PM
已删除: Despite the quantified relationship between S_{X_AI} and S_{X_CDNC}, we suggest that CDNC should be used broadly to estimate precipitation susceptibility compared to AI given the following reasons: (1) near-cloud aerosol retrievals would affect aerosol-cloud relationships in satellite observations. For instance, more resent study of Christensen et al., (2017) shown that cloud albedo effect and cloud faction effect forcing both decreased by 40% and 70% respectively after rejecting aerosol samples located within 15 km of the nearest cloud; (2) the difference of S_{X_CDNC} among S_R, S_I and S_{POP} is more obvious since S_{X_CDNC} are much larger than S_{X_AI} (Fig. 1); (3) S_{X_CDNC} is less sensitive to the wet scavenging effect since it does not need aerosol data for calculation; (4) S_{X_CDNC} can be easily compare to parameterization of cloud microphysics in models (e.g., the water conversion rate by autoconversion process (P_{aut}) in GCMs is usually represented as $P_{aut} \sim LWC^{\alpha} \times CDNC^{-\beta}$, where α and β are both constants and LWC is liquid water content (Michibata et al., 2016)).

Acknowledgement

M. Wang was supported by the National Natural Science Foundation of China (41575073 and 41621005) and by the Jiangsu Province Specially-appointed professorship grant, the One Thousand Young Talents Program. MYD08_D3 and MYD04_L2 products are available through LAADS, the Level 1 and Atmosphere Archive and Distribution System (https://ladsweb.modaps.eosdis.nasa.gov). MYD06_L2 and 2B-GEOPROF data, both collocated to CALIOP subtrack, are obtained from ICARE Data and Services Center (http://www.icare.univ-lille1.fr/projects/calxtract/products). 2C-PRECIP-COLUMN and 2C-RAIN-PROFILE data sets are available from CloudSat Data Processing Center

(http://cloudsat.atmos.colostate.edu/data). CAL_LID_L2_05kmALay data is gained from ASDC, Atmospheric Science Data Center (https://eosweb.larc.nasa.gov). AMSR-E/Aqua L2B Global Swath Ocean product can be obtained from NASA Distributed Active Archive Center (DAAC) at NSIDC (http://nsidc.org/daac). We thank Dr. Johannes Quaas and an anonymous reviewer for their constructive comments, which allows us to further improve the manuscript.

References

Anderson, T. L., Charlson, R. J., Winker, D. M., Ogren, J. a. and Holmén, K.: Mesoscale Variations of Tropospheric Aerosols, J. Atmos. Sci., 60(1), 119–136, doi:10.1175/1520-0469(2003)060<0119:MVOTA>2.0.CO;2, 2003.

Bennartz, R.: Global assessment of marine boundary layer cloud droplet number concentration from satellite, J. Geophys. Res., 112, D02201, doi:DOI 10.1029/2006JD007547, 2007.

Bréon, F. M., Vermeulen, A. and Descloitres, J.: An evaluation of satellite aerosol products against sunphotometer measurements, Remote Sens. Environ., 115(12), 3102–3111, doi:10.1016/j.rse.2011.06.017, 2011.

Chand, D., Wood, R., Ghan, S. J., Wang, M., Ovchinnikov, M., Rasch, P. J., Miller, S., Schichtel, B. and Moore, T.: Aerosol optical depth increase in partly cloudy conditions, J. Geophys. Res. Atmos., 117(17), doi:10.1029/2012JD017894, 2012.

Boucher, O., Randall, D., Artaxo, P., Bretherton, C., Feingold, G., Forster, P., Kerminen, V.-M., Kondo, Y., Liao, H., Lohmann, U., Rasch, P., Satheesh, S. K., Sherwood, S., Stevens, B., and Zhang, X. Y.: Clouds and Aerosols, in: Climate Change 2013: The Phys- ical Science Basis. Contribution ofWorking Group I to the Fifth Assessment Report of the Intergovernmental Panel on Climate Change, edited by: Stocker, T. F., Qin, D., Plattner, G.-K., Tignor, M., Allen, S. K., Boschung, J., Nauels, A., Xia, Y., Bex V., and Midgley, P. M., Cambridge University Press, Cambridge, United Kingdom and New York, NY, USA, 2013.

Chen, Y.-C., Christensen, M. W., Stephens, G. L. and Seinfeld, J. H.: Satellite-based estimate of global aerosol-cloud radiative forcing by marine warm clouds, Nat. Geosci., 7(9), 643–646, doi:10.1038/ngeo2214, 2014.

Cho, H.-M., Zhang, Z., Meyer, K., Lebsock, M., Platnick, S., Ackerman, A. S., Di Girolamo, L., C.-Labonnote, L., Cornet, C., Riedi, J. and Holz, R. E.: Frequency and causes of failed MODIS cloud property retrievals for liquid phase clouds over global oceans, J. Geophys. Res. Atmos., 120(9), 4132–4154, doi:10.1002/2015JD023161, 2015.

Christensen, M. W., Neubauer, D., Poulsen, C., Thomas, G., McGarragh, G., Povey, A. C., Proud, S. and Grainger, R. G.: Unveiling aerosol-cloud interactions Part 1: Cloud contamination in satellite products enhances the aerosol indirect forcing estimate, Atmos. Chem. Phys. Discuss., 20(May), 1–21, doi:10.5194/acp-2017-450, 2017.

Comstock, K. K., Wood, R., Yuter, S. E. and Bretherton, C. S.: Reflectivity and rain rate in and below drizzling stratocumulus, Q. J. R. Meteorol. Soc., 130, 2891–2918, doi:10.1256/qj.03.187, 2004.

Costantino, L. and Bréon, F. M.: Analysis of aerosol-cloud interaction from multi-sensor satellite observations, Geophys.

Res. Lett., 37(11), 1–5, doi:10.1029/2009GL041828, 2010.

Duong, H. T., Sorooshian, A. and Feingold, G.: Investigating potential biases in observed and modeled metrics of aerosol-cloud-precipitation interactions, Atmos. Chem. Phys., 11(9), 4027–4037, doi:10.5194/acp-11-4027-2011, 2011.

Feingold, G. and Siebert, H.: Cloud-Aerosol Interactions from the Micro to the Cloud Scale, MIT Press. Cambridge, Mass, 319–338, 2009.

Feingold, G., McComiskey, A., Rosenfeld, D. and Sorooshian, A.: On the relationship between cloud contact time and precipitation susceptibility to aerosol, J. Geophys. Res. Atmos., 118(18), 10544–10554, doi:10.1002/jgrd.50819, 2013.

Ghan, S., Wang, M., Zhang, S., Ferrachat, S., Gettelman, A., Griesfeller, J., Kipling, Z., Lohmann, U., Morrison, H., Neubauer, D., Partridge, D. G., Stier, P., Takemura, T., Wang, H. and Zhang, K.: Challenges in constraining anthropogenic aerosol effects on cloud radiative forcing using present-day spatiotemporal variability, Proc. Natl. Acad. Sci., 113(21), 5804–5811, doi:10.1073/pnas.1514036113, 2016.

Greenwald, T. J.: A 2 year comparison of AMSR-E and MODIS cloud liquid water path observations, Geophys. Res. Lett., 36(20), 2–7, doi:10.1029/2009GL040394, 2009.

Greenwald, T. J., L'Ecuyer, T. S. and Christopher, S. A.: Evaluating specific error characteristics of microwave-derived cloud liquid water products, Geophys. Res. Lett., 34(22), L22807, doi:10.1029/2007GL031180, 2007.

Gryspeerdt, E., Quaas, J. and Bellouin, N.: Constraining the aerosol influence on cloud fraction, J. Geophys. Res. Atmos., 121(7), 3566–3583, doi:10.1002/2015JD023744, 2016.

Haynes, J. M., L'Ecuyer, T. S., Stephens, G. L., Miller, S. D., Mitrescu, C., Wood, N. B. and Tanelli, S.: Rainfall retrieval over the ocean with spaceborne W-band radar, J. Geophys. Res. Atmos., 114, D00A22, doi:10.1029/2008JD009973, 2009.

Hill, A. A., Shipway, B. J. and Boutle, I. A.: How sensitive are aerosol-precipitation interactions to the warm rain representation?, J. Adv. Model. Earth Syst., 7(3), 987–1004, doi:10.1002/2014MS000422, 2015.

Horváth, Á. and Gentemann, C.: Cloud-fraction-dependent bias in satellite liquid water path retrievals of shallow, non-precipitating marine clouds, Geophys. Res. Lett., 34(22), L22806, doi:10.1029/2007GL030625, 2007.

Hubanks, P., Platnick, S., King, M. and Ridgway, B.: MODIS Atmosphere L3 Gridded Product Algorithm Theoretical Basis Document (ATBD) & Users Guide,Collection 006,Version 4.2., NASA-GSFC, 1, 2016.

Jung, E., Albrecht, B. A., Sorooshian, A., Zuidema, P. and Jonsson, H. H.: Precipitation susceptibility in marine stratocumulus and shallow cumulus from airborne measurements, Atmos. Chem. Phys., 16(17), 11395–11413, doi:10.5194/acp-16-11395-2016, 2016.

Kaufman, Y. J., Tanré, D., Remer, L. A., Vermote, E. F., Chu, A. and Holben, B. N.: Operational remote sensing of tropospheric aerosol over land from EOS moderate resolution imaging spectroradiometer, J. Geophys. Res., 102(D14), 17051–17067, doi:10.1029/96JD03988, 1997.

Kim, M. H., Kim, S. W., Yoon, S. C. and Omar, A. H.: Comparison of aerosol optical depth between CALIOP and

MODIS-Aqua for CALIOP aerosol subtypes over the ocean, J. Geophys. Res. Atmos., 118(23), 13241–13252, doi:10.1002/2013JD019527, 2013.

King, J. M., Kummerow, C. D., van den Heever, S. C. and Igel, M. R.: Observed and Modeled Warm Rainfall Occurrence and Its Relationships with Cloud Macrophysical Properties, J. Atmos. Sci., 72(11), 4075–4090, doi:10.1175/JAS-D-14-0368.1, 2015.

Kittaka, C., Winker, D. M., Vaughan, M. A., Omar, A. and Remer, L. A.: Intercomparison of column aerosol optical depths from CALIPSO and MODIS-Aqua, Atmos. Meas. Tech., 4(2), 131–141, doi:10.5194/amt-4-131-2011, 2011.

Klein, S. A. and Hartmann, D. L.: The seasonal cycle of low stratiform clouds, J. Clim., 6(8), 1587–1606, doi:10.1175/1520-0442(1993)006<1587:TSCOLS>2.0.CO;2, 1993.

Koren, I., Dagan, G. and Altaratz, O.: From aerosol-limited to invigoration of warm convective clouds., Science, 344(6188), 1143–6, doi:10.1126/science.1252595, 2014.

Kubar, T. L., Hartmann, D. L. and Wood, R.: Understanding the Importance of Microphysics and Macrophysics for Warm Rain in Marine Low Clouds. Part I: Satellite Observations, J. Atmos. Sci., 66(10), 2953–2972, doi:10.1175/2009JAS3071.1, 2009.

L'Ecuyer, T. S. and Jiang, J. H.: Touring the atmosphere aboard the A-Train, Phys. Today, 63(7), 36–41, doi:10.1063/1.3653856, 2010.

L'Ecuyer, T. S., Berg, W., Haynes, J., Lebsock, M. and Takemura, T.: Global observations of aerosol impacts on precipitation occurrence in warm maritime clouds, J. Geophys. Res. Atmos., 114(9), 1–15, doi:10.1029/2008JD011273, 2009.

Lebsock, M. D. and L'Ecuyer, T. S.: The retrieval of warm rain from CloudSat, J. Geophys. Res. Atmos., 116(20), 1–14, doi:10.1029/2011JD016076, 2011.

Levy, R. C., Mattoo, S., Munchak, L. A., Remer, L. A., Sayer, A. M., Patadia, F. and Hsu, N. C.: The Collection 6 MODIS aerosol products over land and ocean, Atmos. Meas. Tech., 6(11), 2989–3034, doi:10.5194/amt-6-2989-2013, 2013.

Ma, X., Bartlett, K., Harmon, K. and Yu, F.: Comparison of AOD between CALIPSO and MODIS: Significant differences over major dust and biomass burning regions, Atmos. Meas. Tech., 6(9), 2391–2401, doi:10.5194/amt-6-2391-2013, 2013.

Mann, J. A. L., Chiu, J. C., Hogan, R. J., Oconnor, E. J., Lecuyer, T. S., Stein, T. H. M. and Jefferson, A.: Aerosol impacts on drizzle properties in warm clouds from ARM Mobile Facility maritime and continental deployments, J. Geophys. Res., 119(7), 4136–4148, doi:10.1002/2013JD021339, 2014.

Marchand, R., Mace, G. G., Ackerman, T. and Stephens, G.: Hydrometeor detection using Cloudsat - An earth-orbiting 94-GHz cloud radar, J. Atmos. Ocean. Technol., 25(4), 519–533, doi:10.1175/2007JTECHA1006.1, 2008.

McComiskey, A. and Feingold, G.: The scale problem in quantifying aerosol indirect effects, Atmos. Chem. Phys., 12(2), 1031–1049, doi:10.5194/acp-12-1031-2012, 2012.

Michibata, T., Suzuki, K., Sato, Y. and Takemura, T.: The source of discrepancies in aerosol--cloud--precipitation interactions between GCM and A-Train retrievals, Atmos. Chem. Phys., 16(23), 15413–15424, doi:10.5194/acp-16-15413-2016, 2016.

Miller, D. J., Zhang, Z., Ackerman, A. S., Platnick, S. and Baum, B. A.: The impact of cloud vertical profile on liquid water path retrieval based on the bispectral method: A theoretical study based on large-eddy simulations of shallow marine boundary layer clouds, J. Geophys. Res. Atmos., 121(8), 4122–4141, doi:10.1002/2015JD024322, 2016.

Mülmenstädt, J., Sourdeval, O., Delanoë, J. and Quaas, J.: Frequency of occurrence of rain from liquid-, mixed-, and ice-phase clouds derived from A-Train satellite retrievals, Geophys. Res. Lett., 42(15), 6502–6509, doi:10.1002/2015GL064604, 2015.

Nakajima, T., Higurashi, A., Kawamoto, K. and Penner, J. E.: A possible correlation between satellite-derived cloud and aerosol microphysical parameters, Geophys. Res. Lett., 28(7), 1171–1174, doi:10.1029/2000GL012186, 2001.

Nam, C. C. W. and Quaas, J.: Geographically versus dynamically defined boundary layer cloud regimes and their use to evaluate general circulation model cloud parameterizations, Geophys. Res. Lett., 40(18), 4951–4956, doi:10.1002/grl.50945, 2013.

Platnick, S. and Twomey, S.: Determining the susceptibility of cloud albedo to changes in droplet concentration with the Advanced Very High Resolution Spectrometer, J. Appl. Meteorol., 33(3), 334–347, doi:10.1175/1520-0450(1994)033<0334:DTSOCA>2.0.CO;2, 1994.

Platnick, S., King, M. D., Ackerman, S. A., Menzel, W. P., Baum, B. A., Riédi, J. C. and Frey, R. A.: The MODIS cloud products: Algorithms and examples from terra, IEEE Trans. Geosci. Remote Sens., 41(2 PART 1), 459–472, doi:10.1109/TGRS.2002.808301, 2003.

Platnick, S., Meyer, K. G., King, M. D., Wind, G., Amarasinghe, N., Marchant, B., Arnold, G. T., Zhang, Z., Hubanks, P. A., Holz, R. E., Yang, P., Ridgway, W. L. and Riedi, J.: The MODIS Cloud Optical and Microphysical Products: Collection 6 Updates and Examples from Terra and Aqua, IEEE Trans. Geosci. Remote Sens., 55(1), 502–525, doi:10.1109/TGRS.2016.2610522, 2017.

Quaas, J., Boucher, O. and Lohmann, U.: Constraining the total aerosol indirect effect in the LMDZ and ECHAM4 GCMs using MODIS satellite data, Atmos. Chem. Phys., 6(4), 947–955, doi:10.5194/acp-6-947-2006, 2006.

Seethala, C. and Horváth, Á.: Global assessment of AMSR-E and MODIS cloud liquid water path retrievals in warm oceanic clouds, J. Geophys. Res. Atmos., 115(13), 1–19, doi:10.1029/2009JD012662, 2010.

Sorooshian, A., Feingold, G., Lebsock, M. D., Jiang, H. and Stephens, G. L.: On the precipitation susceptibility of clouds to aerosol perturbations, Geophys. Res. Lett., 36, L13803, doi:10.1029/2009GL038993, 2009.

Stephens, G. L., Vane, D. G., Boain, R. J., Mace, G. G., Sassen, K., Wang, Z., Illingworth, A. J., O'Connor, E. J., Rossow, W. B., Durden, S. L., Miller, S. D., Austin, R. T., Benedetti, A. and Mitrescu, C.: The cloudsat mission and the A-Train: A

new dimension of space-based observations of clouds and precipitation, Bull. Am. Meteorol. Soc., 83(12), 1771–1790, doi:10.1175/BAMS-83-12-1771, 2002.

Szczodrak, M., Austin, P. H. and Krummel, P. B.: Variability of optical depth and effective radius in marine stratocumulus clouds, J. Atmos. Sci., 58(19), 2912–2926, doi:10.1175/1520-0469(2001)058<2912:VOODAE>2.0.CO;2, 2001.

Tackett, J. L. and Di Girolamo, L.: Enhanced aerosol backscatter adjacent to tropical trade wind clouds revealed by satellite-based lidar, Geophys. Res. Lett., 36(14), 1–5, doi:10.1029/2009GL039264, 2009.

Tanré, D., Kaufman, Y. J., Herman, M. and Mattoo, S.: Remote sensing of aerosol properties over oceans using the MODIS/EOS spectral radiances, J. Geophys. Res., 102(D14), 16971–16988, doi:10.1029/96JD03437, 1997.

Terai, C. R., Wood, R., Leon, D. C. and Zuidema, P.: Does precipitation susceptibility vary with increasing cloud thickness in marine stratocumulus, Atmos. Chem. Phys., 12(10), 4567–4583, doi:10.5194/acp-12-4567-2012, 2012.

Terai, C. R., Wood, R. and Kubar, T. L.: Satellite estimates of precipitation susceptibility in low-level marine stratiform clouds, J. Geophys. Res. Atmos., 120(17), 8878–8889, doi:10.1002/2015JD023319, 2015.

Vaughan, M. a, Young, S., Winker, D. M., Powell, K., Omar, a, Liu, Z., Hu, Y. and Hostetler, C.: Fully automated analysis of space-based lidar data: an overview of the CALIPSO retrieval algorithms and data products, Proc. SPIE, 5575, 16–30, doi:10.1117/12.572024, 2004.

Wang, M., Ghan, S., Liu, X., L'Ecuyer, T. S., Zhang, K., Morrison, H., Ovchinnikov, M., Easter, R., Marchand, R., Chand, D., Qian, Y. and Penner, J. E.: Constraining cloud lifetime effects of aerosols using A-Train satellite observations, Geophys. Res. Lett., 39, L15709, doi:10.1029/2012GL052204, 2012.

Wentz, F. and Meissner, T.: AMSR Ocean Algorithm Theoretical Basis Document (ATBD), RSS Tech.Doc, Santa Rosa,Calif., 2000.

Wentz, F.. and Meissner, T.: AMSR-E/Aqua L2B Global Swath Ocean Products derived from Wentz Algorithm. Version 2. Boulder, Colorado USA: NASA National Snow and Ice Data Center Distributed Active Archive Center. doi: 10.5067/AMSR-E/AE_OCEAN.002,2004.

Wood, R.: Drizzle in Stratiform Boundary Layer Clouds. Part II: Microphysical Aspects, J. Atmos. Sci., 62(9), 3034–3050, doi:10.1175/JAS3530.1, 2005.

Wood, R. and Hartmann, D. L.: Spatial variability of liquid water path in marine low cloud: The importance of mesoscale cellular convection, J. Clim., 19(9), 1748–1764, doi:10.1175/JCLI3702.1, 2006.

Young, S. A. and Vaughan, M. A.: The Retrieval of Profiles of Particulate Extinction from Cloud-Aerosol Lidar Infrared Pathfinder Satellite Observations (CALIPSO) Data: Algorithm Description, J. Atmos. Ocean. Technol., 26(6), 1105–1119, doi:10.1175/2008JTECHA1221.1, 2009.

Zhang, S., Wang, M., J. Ghan, S., Ding, A., Wang, H., Zhang, K., Neubauer, D., Lohmann, U., Ferrachat, S., Takeamura, T., Gettelman, A., Morrison, H., Lee, Y., T. Shindell, D., G. Partridge, D., Stier, P., Kipling, Z. and Fu, C.: On the

characteristics of aerosol indirect effect based on dynamic regimes in global climate models, Atmos. Chem. Phys., 16(5), 2765–2783, doi:10.5194/acp-16-2765-2016, 2016.

Zhang, Z. and Platnick, S.: An assessment of differences between cloud effective particle radius retrievals for marine water clouds from three MODIS spectral bands, J. Geophys. Res. Atmos., 116(20), doi:10.1029/2011JD016216, 2011.

Table 1. The summary of previous satellite studies for estimating precipitation susceptibility.

Studies	Rain variables	Aerosol Proxies	Thresholds	Behavior	Satellite datasets
Sorooshian et al., 2009	I	AI	surface 1mm h^{-1}	S_I:↗↘	2C-PRECIP-COLUMN AMSR-E L2B-Ocean MYD08-D3
Wang et al., 2012	POP	AI	rain certain[a]	S_{POP}<0.2	2C-PRECIP-COLUMN AMSR-E L2B-Ocean MYD08-D3
Terai et al., 2015	R/POP/I	CDNC	-15dBZ of Z_{max}[b]	S_R: ↘ S_{POP}:↘ S_I:↗	2B-GEOPROF MYD06_L2
Michibata et al., 2016	I	CDNC	-15dBZ of Z_{max}[b]	S_I:↗↘	2B-GEOPROF MYD06_L2

[a]Rain certain is a flag of 2C-PRECIP-COLUMN product, which is equivalent to greater than attenuation-corrected reflectivity threshold of 0dBZ.

[b]Z_{max}: the maximum column radar reflectivity from the 2B-GEOPROF product. Symbols of ↗ (↘) represent the increasing (decreasing) trend of susceptibility with increasing LWP.

Table 2. Satellite products employed to estimate aerosol and cloud properties in this study

Parameter	Product	Subset	Horizontal resolution	Sensor	Satellite
AI	MYD08_D3	Aerosol_Optical_Depth_Land_Ocean_Mean	1°	MODIS	AQUA
		Aerosol_AE1_Ocean_JHisto_vs_Opt_Depth			
	MYD04_L2	Optical_Depth_Land_And_Ocean	10km		
		Angstrom_Exponent_1_Ocean			
	CAL_LID_L2_05kmALay	Column_Optical_Depth_Aerosol_532	5km	CALIOP	CALIPSO
		Column_Optical_Depth_Aerosols_1064			
CDNC/LWP	MYD06_L2[a]	Cloud_Effective_Radius	5km	MODIS	AQUA
		Cloud_Optical_Thickness			
LWP	AE_Ocean_L2B	High_res_cloud	12km	AMSR-E	AQUA
POP/R	2B-GEOPROF[a]	CPR_Cloud_mask	5km	CPR	CloudSat
		Radar_Reflectivity			
	2C-PRECIP-COLUMN	Precip_rate	1.4km×1.7km		
		Precip_flag			
	2C-RAIN-PROFILE	Rain_rate			
		Precip_flag			

[a]The original horizontal resolution of MYD06_L2 and 2B-GEOPROF products is 1km and 1.4km×1.7km, respectively. Since these products both are obtained from caltrack product collocated to CALIOP subtrack, the resolution is resampled to 5km. Detailed information is provided by the website (http://www.icare.univ-lille1.fr/projects/calxtract/products).

Table 3. The LWP weighted-mean values of precipitation susceptibility Sx_y and dlnCDNC/dlnAI over global oceans under different stability regimes. The statistics is based on 2B-GEOPROF/CPR product using cloud base Z-R relationship and -15dBZ threshold.

		S_{R_AI}	S_{I_AI}	S_{POP_AI}	S_{R_CDNC}	S_{I_CDNC}	S_{POP_CDNC}	dlnCDNC/dlnAI
MODIS LWP	global	0.05	-0.02	0.08	0.74	0.47	0.44	0.28
	unstable	-0.04	-0.09	0.04	0.52	0.30	0.26	0.22
	stable	0.22	0.13	0.12	0.84	0.48	0.60	0.30
	midstable	0.01	-0.05	0.07	0.66	0.39	0.35	0.29
AMSR-E LWP	global	0.17	0.07	0.11	0.47	0.16	0.37	0.32
	unstable	0.14	0.06	0.08	0.21	0.04	0.18	0.25
	stable	0.29	0.17	0.15	0.67	0.23	0.55	0.33
	midstable	0.13	0.04	0.10	0.40	0.13	0.29	0.34

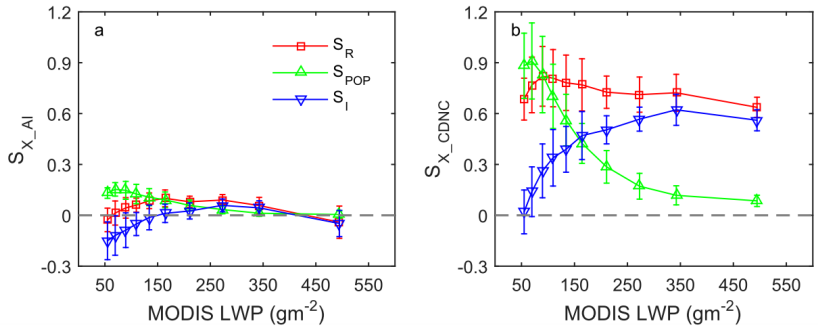

Figure 1. S_{POP}, S_I and S_R as a function of MODIS LWP with (a) AI and (b) CDNC. Red squares, green upward triangles and blue downward triangles stand for S_R, S_{POP} and S_I, respectively. Error bars are based on 95% confidence intervals for the susceptibility estimates. AI is derived from MYD04/MODIS and CDNC is estimated from MYD06/MODIS. Intensity and probability of precipitation are based on 2B-GEOPROF product with -15dBZ threshold. The total amount of data samples for left panel and right panel are about 2.1 and 3.1 million.

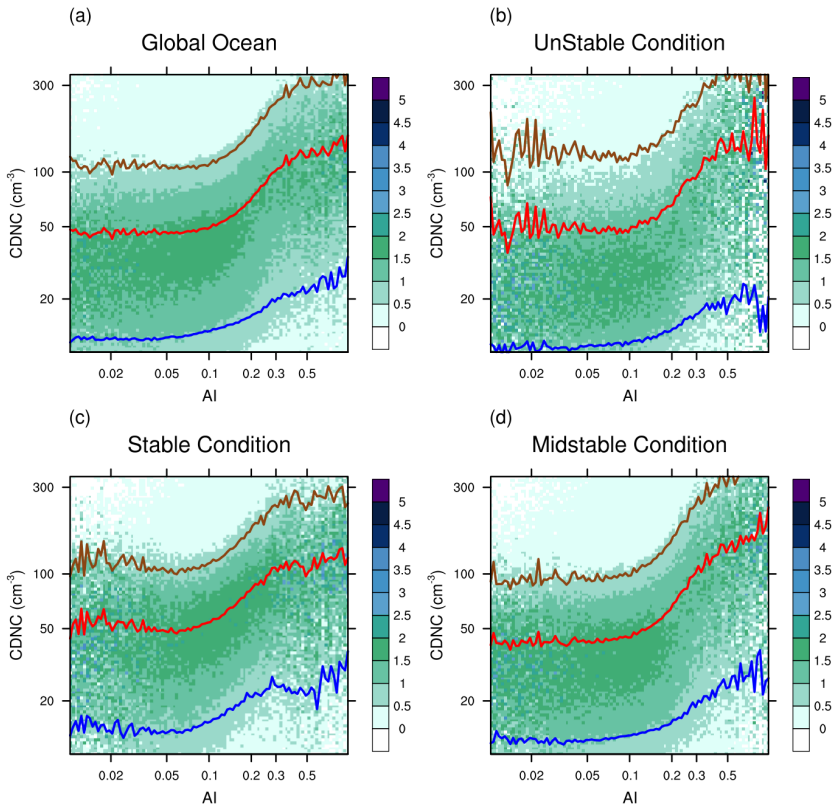

Figure 2. The probability of CDNC under given AI over (a) global ocean, (b) unstable, (c) stable and (d) mid-stable conditions. In each figure, the red line represents change in average CDNC with AI, and the lower and upper lines stand for mean CDNC for 25 percentile and 75 percentile of samples. AI and CDNC are estimated from MYD04 and MYD06, respectively.

Minghuai Wang 2017/12/7 11:39 PM
已删除: . And

Minghuai Wang 2017/12/7 11:39 PM
已删除: blue

Minghuai Wang 2017/12/7 11:39 PM
已删除: chocolate

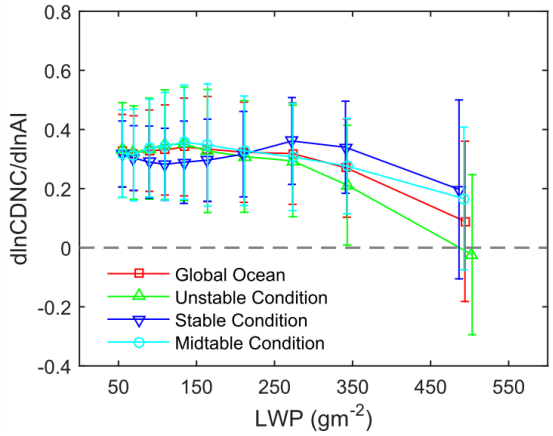

Figure 3. dlnCDNC/dlnAI obtained by linear regression of lnCDNC and lnAI under MODIS LWP bins. Red line denote global ocean. Green, blue and cyan stand for unstable, stable and mid-stable condition, respectively. AI and CDNC are estimated from MYD04 and MYD06.

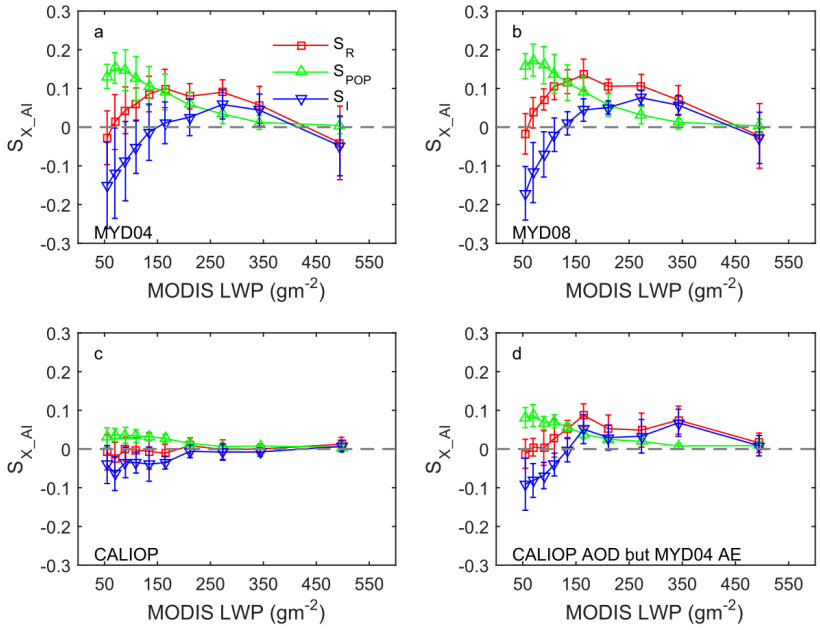

Figure 4. Susceptibilities (S_{X_AI}) as a function of MODIS LWP. Rain product used is the same as Figure 1. AI is derived from (a) MYD04/MODIS, (b) MYD08/MODIS and (c) CAL_LID_L2_05kmALay/CALIOP product. Panel d is the same as panel c but using MYD04 AE.

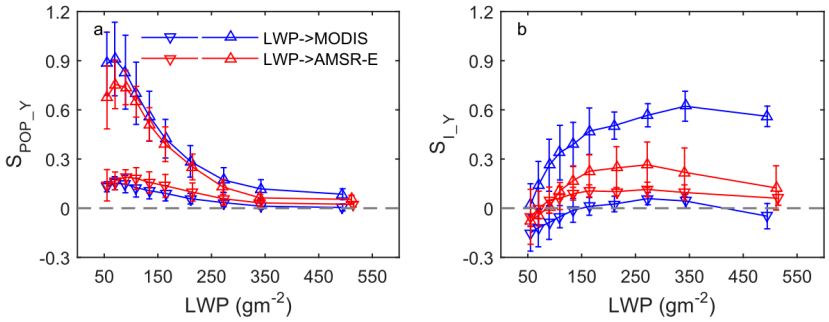

Figure 5. (a) S_{POP_Y} and (b) S_{I_Y} as a function of LWP. The subscript Y denotes different aerosol proxies corresponding to AI (downward triangles) and CDNC (upward triangles). Blue (red) represent LWP derived from MODIS (AMSR-E). Rain product used is the same as Figure 1. AI and CDNC are estimated from MYD04 and MYD06, respectively.

dell 2017/11/28 3:00 PM
已删除: point

dell 2017/11/28 3:01 PM
已删除: square

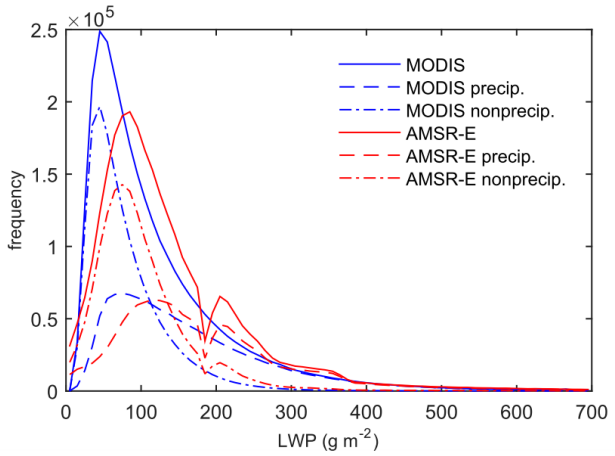

Figure 6. Distribution of frequency of LWP derived from MODIS and AMSR-E under different scenarios, namely, all samples, nonprecipitation and only precipitation samples.

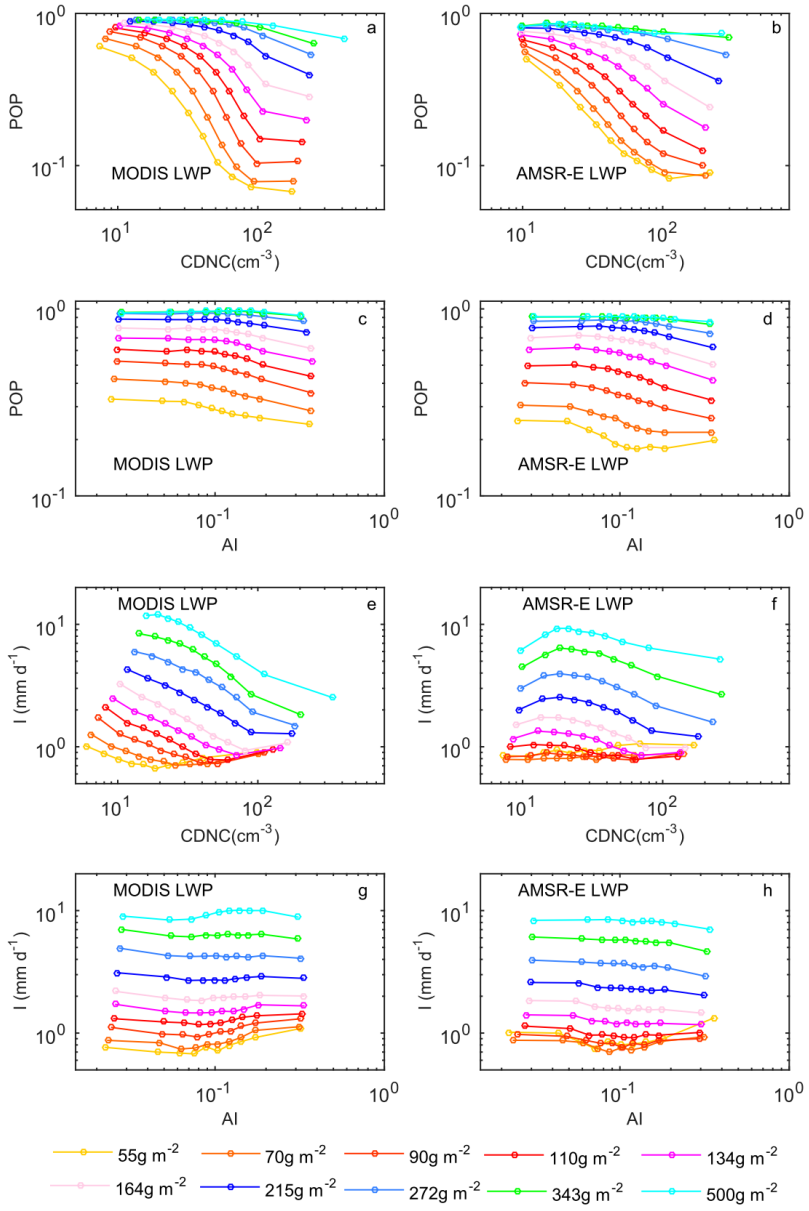

Figure 7. POP and I as a function of CDNC (AI) for each LWP bin obtained from (left) MODIS and (right) AMSR-E. The data used here is the same as Figure 5.

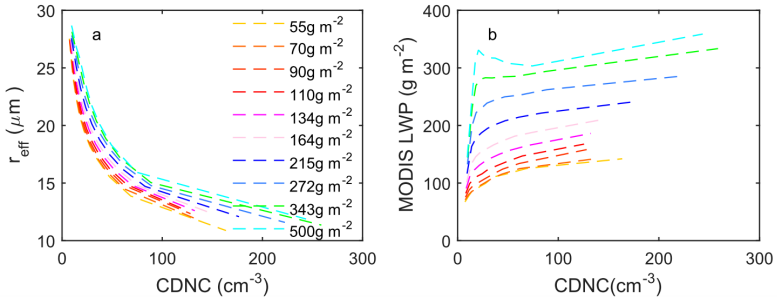

Figure 8. (a) r_{eff} and (b) MODIS LWP as a function of CDNC for each AMSR-E LWP bin. Only rainy samples defined by -15dBZ threshold are used in here. Different color lines represent different AMSR-E bins corresponding to Fig. 7f.

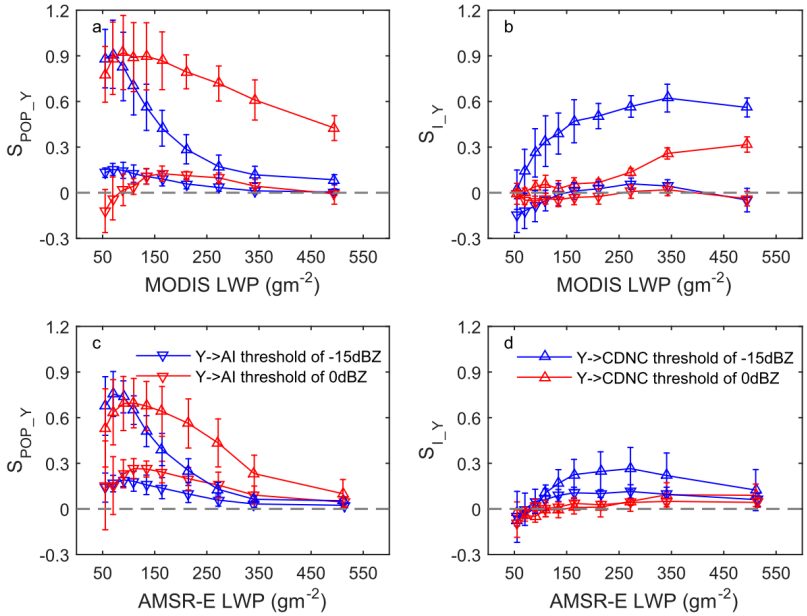

Figure 9. (a, c) S_{POP_Y} and (b, d) S_{I_Y} as a function of LWP. The subscript y denotes different aerosol proxies corresponding to AI (downward triangles) and CDNC (upward triangles). 2B-GEOPROF product is used here. Blue and red symbols represent -15dBZ threshold and 0dBZ threshold, respectively. The top and bottom panels stand for MODIS and AMSR-E LWP, respectively.

dell 2017/11/29 7:07 PM
已删除: point

dell 2017/11/29 7:07 PM
已删除: square

Minghuai Wang 2017/12/5 10:03 PM
已删除: row

Minghuai Wang 2017/12/5 10:03 PM
已删除: .

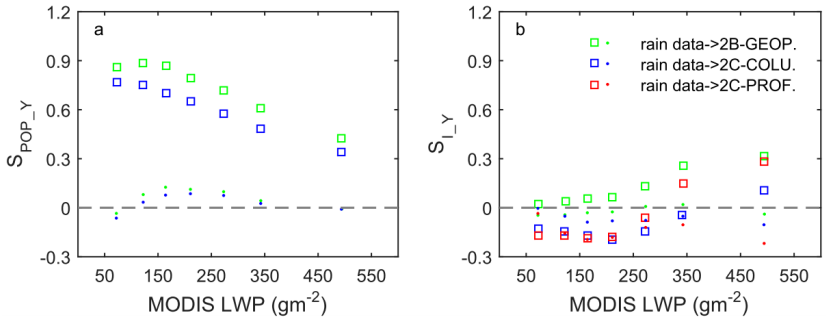

Figure 10. (a) S_{POP_Y} and (b) S_{I_Y} as a function of MODIS LWP. The subscript Y denotes different aerosol proxies corresponding to AI (point) and CDNC (square). Different color symbols stand for different rain products: 2B-GEOPROF (2B-GEOP, green), 2C-PRECIP-COLUMN (2C-COLU, blue) and 2C-RAIN-PROFILE (2C-PROF, red). See text for further details.

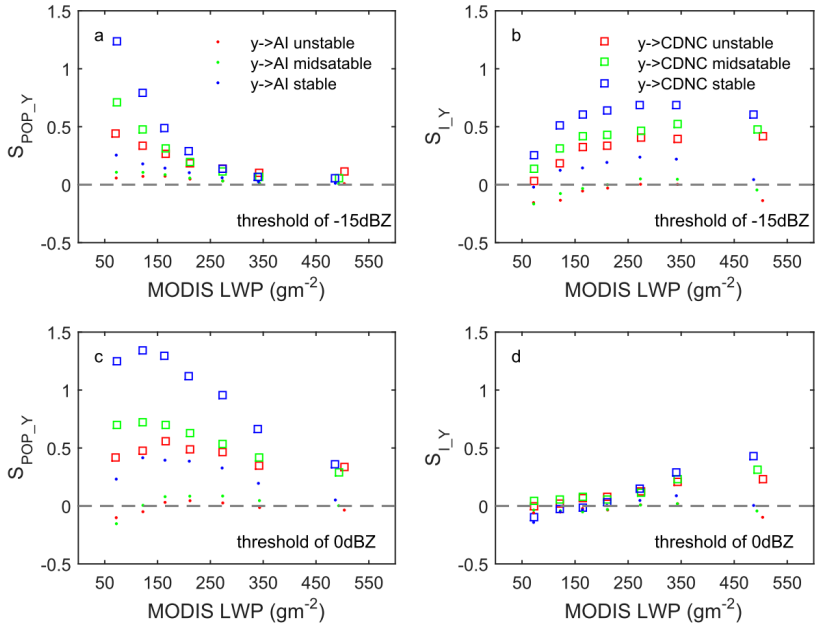

Figure 11. (a, c) S_{POP_Y} and (b, d) S_{I_Y} as a function of MODIS LWP. The subscript y denotes different aerosol proxies corresponding to AI (point) and CDNC (square). Blue, red and green symbols stand for stable, unstable and mid-stable regimes, respectively. Rain data comes from 2B-GEOPROF. The top panels are for results based on the rain threshold of -15 dBZ and the bottom panels are based on the rain threshold of 0 dBZ.

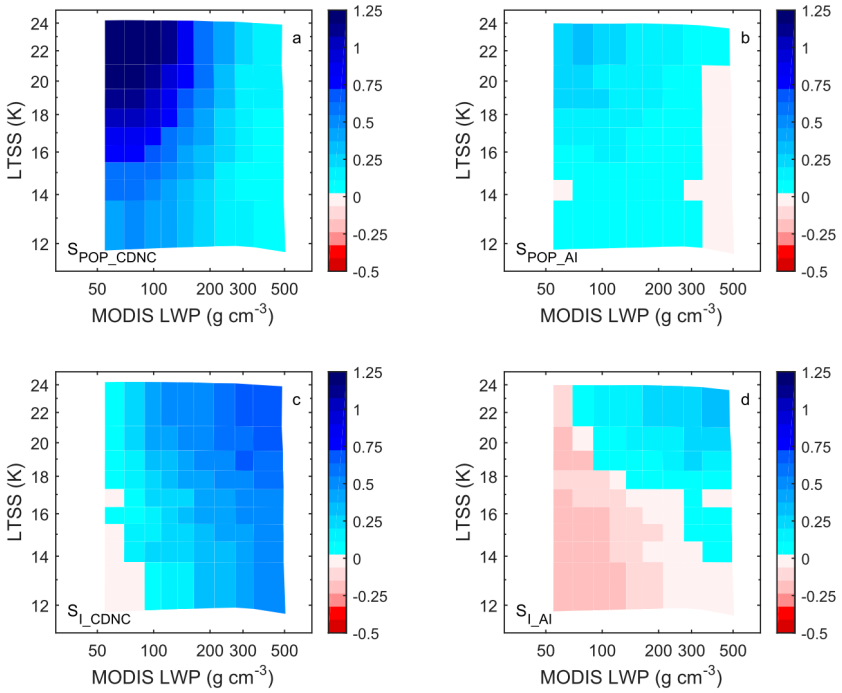

Figure 12. Distribution of (a-b) S_{POP_Y} and (c-d) S_{I_Y} as a function of MODIS LWP and LTSS. Rain data is from 2B-GEOPROF with threshold of -15dBZ. Each LTSS bin contains on average the same amount of pixels.

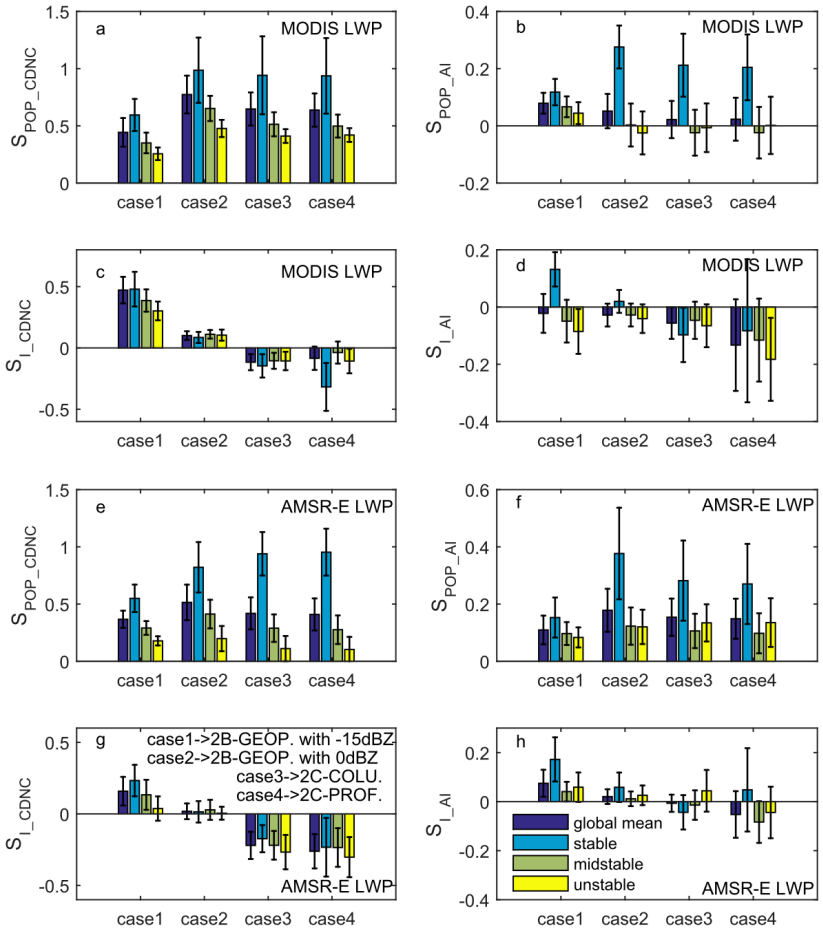

Figure 13. The LWP-weighed mean values of (a-b, e-f) S_{POP} and (c-d, g-h) S_I under different stability regimes for four cases. The case1 and case2 are both based on 2B-GEOPROF product, but use threshold of -15 dBZ and 0 dBZ, respectively. The case3 and case4 use 2C-PRECIP-COLUMN and 2C-RAIN-PROFILE products, respectively. The top two panels use MODIS LWP and the bottom two panels use AMSR-E LWP. Error bars are based on the LWP-weighed mean values of 95% confidence intervals for the susceptibility estimates.

Minghuai Wang 2017/12/7 11:41 PM
批注 [1]: How about error bars?

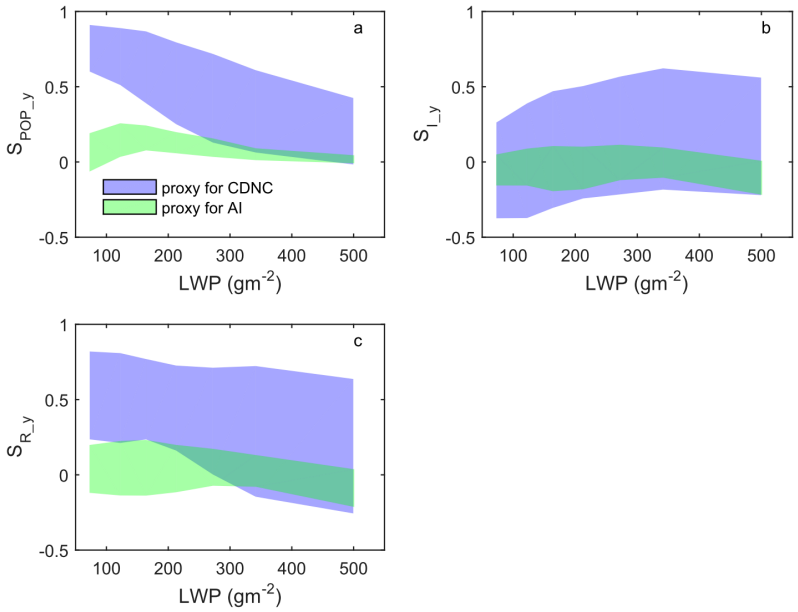

Figure 14. (a) S_{POP_Y}, (b) S_{I_Y} and (c) S_{R_Y} as a function of LWP. The subscript y denotes different aerosol proxies corresponding to AI (light green) and CDNC (light blue). Shade areas show the range of precipitation susceptibility from different rain products (same as the Fig. 10) and different LWP products (MODIS and AMSR-E).